National Library of Canada
Bibliothèque nationale du Canada

Canadian Theses Service
Service des thèses canadiennes

Ottawa, Canada
K1A 0N4

NOTICE

The quality of this microform is heavily dependent upon the quality of the original thesis submitted for microfilming. Every effort has been made to ensure the highest quality of reproduction possible.

If pages are missing, contact the university which granted the degree.

Some pages may have indistinct print especially if the original pages were typed with a poor typewriter ribbon or if the university sent us an inferior photocopy.

Previously copyrighted materials (journal articles, published tests, etc.) are not filmed.

Reproduction in full or in part of this microform is governed by the Canadian Copyright Act, R.S.C. 1970, c. C-30.

AVIS

La qualité de cette microforme dépend grandement de la qualité de la thèse soumise au microfilmage. Nous avons tout fait pour assurer une qualité supérieure de reproduction.

S'il manque des pages, veuillez communiquer avec l'université qui a conféré le grade.

La qualité d'impression de certaines pages peut laisser à désirer, surtout si les pages originales ont été dactylographiées à l'aide d'un ruban usé ou si l'université nous a fait parvenir une photocopie de qualité inférieure.

Les documents qui font déjà l'objet d'un droit d'auteur (articles de revue, tests publiés, etc.) ne sont pas microfilmés.

La reproduction, même partielle, de cette microforme est soumise à la Loi canadienne sur le droit d'auteur, SRC 1970, c. C-30.

NL-339 (r. 88/04)

Canada

THE UNIVERSITY OF ALBERTA

Combined effects of stress and velocity of flow on corrosion potential of 1025 steel

by

Henryk Skrzypek

(C)

A THESIS

SUBMITTED TO THE FACULTY OF GRADUATE STUDIES AND RESEARCH

IN PARTIAL FULFILMENT OF THE REQUIREMENTS FOR THE DEGREE

OF Master of Science

IN

Metallurgical Engineering

Department of Mining, Metallurgical and Petroleum Engineering

EDMONTON, ALBERTA

FALL, 1988.

Permission has been granted to the National Library of Canada to microfilm this thesis and to lend or sell copies of the film.

The author (copyright owner) has reserved other publication rights, and neither the thesis nor extensive extracts from it may be printed or otherwise reproduced without his/her written permission.

L'autorisation a été accordée à la Bibliothèque nationale du Canada de microfilmer cette thèse et de prêter ou de vendre des exemplaires du film.

L'auteur (titulaire du droit d'auteur) se réserve les autres droits de publication; ni la thèse ni de longs extraits de celle-ci ne doivent être imprimés ou autrement reproduits sans son autorisation écrite.

ISBN 0-315-45530-6

THE UNIVERSITY OF ALBERTA

RELEASE FORM

NAME OF AUTHOR Henryk Skrzypek

TITLE OF THESIS Combined effects of stress and velocity of flow on corrosion potential of 1025 steel

DEGREE FOR WHICH THESIS WAS PRESENTED Master of Science

YEAR THIS DEGREE GRANTED FALL, 1988.

Permission is hereby granted to THE UNIVERSITY OF ALBERTA LIBRARY to reproduce single copies of this thesis and to lend or sell such copies for private, scholarly or scientific research purposes only.

The author reserves other publication rights, and neither the thesis nor extensive extracts from it may be printed or otherwise reproduced without the author's written permission.

(SIGNED) Henryk Skrzypek

PERMANENT ADDRESS:

5812 - 113 str.

Edmonton, Alberta

T6H 1G5

DATED April 20 1988

THE UNIVERSITY OF ALBERTA

FACULTY OF GRADUATE STUDIES AND RESEARCH

The undersigned certify that they have read, and recommend to the Faculty of Graduate Studies and Research, for acceptance, a thesis entitled Combined effects of stress and velocity of flow on corrosion potential of 1025 steel submitted by Henryk Skrzypek in partial fulfilment of the requirements for the degree of Master of Science in Metallurgical Engineering.

Samuel A. Bradford

Supervisor

Date. May 6, 1988

Dedication

To my parents, my wife Halina and my children Dorota and Magdalena.

Abstract

Precise measurements of the steady state corrosion potential of stressed 1025 steel electrodes in stagnant and flowing 3% NaCl solution were done to investigate the influence of velocity of flow on electrochemical response to stress energy.

Continuous curves of potential vs. stress for loading and unloading below the elastic limit and for loading beyond the yield point were obtained.

The results of the tests have shown that elastic strain energy shifts the corrosion potential linearly in the noble direction. Increasing velocity of flow reduces the slope of the linear change. A noble shift, contradictory to theoretical prediction, might be explained by the presence of compressive stresses in the surface of the mechanically prepared sample but no definite conclusion can be made.

In loading beyond the elastic limit an increased velocity of flow increased reactivity of the freshly exposed deformed surface of the bare metal. The corrosion film needed less deformation to break at higher velocity ranges.

Acknowledgements

I would like to express my sincere gratitude to my supervisor Dr. S.A. Bradford for his guidance, encouragement and help.

I would also like to thank my brother Dr. S. Skrzypek for some of the tests done as a part of this study.

My appreciation is also extended to the technical staff in the department for their help, specifically Mrs. T. Barker, Mr. D. Booth, Mr. B. Smith and Mr. R. Stefaniuk.

Also, I would like to thank Mr. V. Voruganti and Mr. E. Leigh for their support and help.

List of tables

Table		Page
1.	Chemical composition of the test steel.	42
2.	Mechanical properties of the test steel.	43
3.	The results of the X-ray data search.	45
4.	Velocities of flow and corresponding Reynolds numbers.	47

List of figures

Figure		Page
1.	The electrode potential transient of copper in distilled water.	61
2.	Effect of velocity of flow on the electrochemical behaviour of metal corroding with a diffusion controlled cathodic reaction.	61
3.	Polarization curves for 1025 steel in 3% NaCl solution at room temperature.	62
4.	Microstructure of 1025 steel magnified 200 times.	63
5.	The test specimen.	63
6.	The test corrosion cell.	64
7.	Schematic drawing of experimental apparatus.	65
8.	Stability of the corrosion potential at steady state conditions in stagnant solution.	66
9.	Stability of the corrosion potential at steady state conditions in flowing solution at random velocity.	66
10.	Effect of velocity of flow on corrosion potential and the slope of the potential/stress curves.	67
11.	Effect of tensile stress on corrosion potential of 1025 steel in 3% NaCl solution.(Velocity of flow: 0.0 m/s, rest potential: -779.5 mV)	68
12.	Effect of tensile stress on corrosion potential of 1025 steel in 3% NaCl solution.(Velocity of flow: 0.1 m/s, rest potential: -766.0 mV)	69

13. Effect of tensile stress on corrosion potential of 1025 steel in 3% NaCl solution.(Velocity of flow: 0.25 m/s, rest potential: -758.9 mV) 70
14. Effect of tensile stress on corrosion potential of 1025 steel in 3% NaCl solution.(Velocity of flow: 0.5 m/s, rest potential: -754.7 mV) 71
15. Effect of tensile stress on corrosion potential of 1025 steel in 3% NaCl solution.(Velocity of flow: 1.5 m/s, rest potential: -747.7 mV) 72
16. Effect of tensile stress on corrosion potential of 1025 steel in 3% NaCl solution.(Velocity of flow: 2.5 m/s, rest potential: -744.5 mV) 73
17. Effect of tensile stress on corrosion potential of 1025 steel in 3% NaCl solution.(Velocity of flow: 3.5 m/s, rest potential: -740.0 mV) 74
18. Effect of tensile stress on corrosion potential of 1025 steel in 3% NaCl solution at various velocities of flow. 75
19. Potential change during the first straining cycle at various flow rates. 76
20. Potential change during the second straining cycle at various flow rates. 77
21. Potential change during the third straining cycle at various flow rates. 78
22. Potential change during the fourth straining cycle at various flow rates. 79

23. Potential change during the fifth straining cycle at various flow rates. 80

24. Potential decay curves for 1025 steel in 3% NaCl solution at various velocities of flow for third straining cycle. 81

Table of Contents

Chapter — Page

1. INTRODUCTION 1

2. EFFECT OF STRESS AND STRAIN ON ELECTRODE POTENTIAL ...3

2.1 Theory 3

2.1.1 Stress effect 3

2.1.2 Plastic strain effect. 8

2.2 Literature review on the effect of stress, cold work and continuous straining upon potential of metal 17

2.2.1 Effect of stress 17

2.2.2 Effect of cold work 19

2.2.3 Effect of continuous straining 20

2.3 Proposed theories of stress and strain effects ..23

2.3.1 Stress effect. 23

2.3.2 Cold work effect. 25

2.3.3 Straining electrode effect. 28

3. EFFECT OF VELOCITY OF FLOW ON ELECTRODE POTENTIAL ...30

3.1 Theory 30

3.2 Literature review 37

4. EXPERIMENT, RESULTS AND CONCLUSIONS 42

4.1 Material, solution and initial measurements 42

4.1.1 Material. 42

4.1.2 Solution 43

4.1.3 Corrodibility of the steel in the stagnant solution. 44

4.1.4 The quality of the film formed at a potential above the activation polarization range. 44

4.1.5 The microstructure of the test steel 45

4.1.6 Measurements of residual stresses in the surface layer 46

4.2 Program and procedure of the test. 47

4.2.1 Tests in elastic loading range. 47

4.2.2 Tests in plastic loading range. 47

4.2.3 Specimen preparation and instrumentation setup. 48

4.2.4 Test procedure. 49

4.3 Results and discussion 50

4.3.1 Results obtained from elastic loading 50

4.3.2 Results obtained from plastically straining electrode. 54

4.4 Conclusions 59

REFERENCES 82

APPENDIX A. Calculation of temperature change due to thermoelastic effect 87

APPENDIX B. Thermodynamic calculation of potential change of stressed steel. 88

APPENDIX C. Determining the corrosion rate of 1025 steel in 3% NaCl solution. 90

1. INTRODUCTION

Most metals and alloys in practical use are exposed to a corrosion environment while under applied or residual stress, or a combination of both of the two stresses.

These stresses can be of static or dynamic nature. Their magnitude can exceed the metal's elastic limit if the stress raisers such as corrosion pits, crevice corrosion, or pre-existing or newly formed microcracks or voids are present. Protruding slip steps in a yielding metal break the protection film and are subject to local attack.

These environment-assisted failure processes have previously been studied in terms of measuring electrochemical parameters such as potential and current, but only in stagnant solutions. Numerous works by many authors have been done in which different factors were considered, such as surface preparation, composition of metal, solution and strain rate.

Stressed and strained electrodes were exposed, in most cases, to flowing liquids which until recently were not considered as a variable which may affect environmental failure. Recently, some research people have been trying to test susceptibility of some alloys to stress corrosion cracking in flowing solutions. Opinions from two recent publications are worth mentioning. Choi, Beck, Szklarska-Smialowska and Macdonald' wrote:

"One variable that intuitively could have a large effect

upon the susceptibility of alloys to SCC in aggressive environments is fluid flow."

Hickling[3] wrote:

"Choi, et al.,are to be congratulated upon pointing out the considerable effects of fluid flow on stress corrosion cracking (SCC) in high temperature water, at least in the slow strain rate test. This is probably of considerable practical importance and has been ignored in much mechanistic works."

Concern about the effect of flowing solution on susceptibility of metals to environmental fracture points to the necessity of studying this effect on corrodibility of freshly exposed metal surfaces of a straining electrode.

This thesis is the first attempt to evaluate the effect of flow rate on potential change during stressing and straining of an electrode.

2. EFFECT OF STRESS AND STRAIN ON ELECTRODE POTENTIAL

2.1 Theory

2.1.1 Stress effect

The free energy change is related to the electrochemical reaction potential by equation 1.

$$\Delta G = - nFE \qquad (1)$$

where:

ΔG = change of Gibbs free energy of the electrode.

n = valence of the ion involved in the electrochemical reaction.

F = the Faraday constant.

E = the potential of the single electrode.

When the elastically-stressed system performs a reversible isothermal process, the amount of the work[3] is

$$dW = - E\varepsilon d\varepsilon \qquad (2)$$

where:

dW = change in performed work related to the change in strain.

ϵ = elastic strain.

E = modulus of elasticity.

$d\epsilon$= change in strain.

The negative of the total work performed reversibly at constant temperature from a state of zero, that is when its strain is equal to the thermal strain, is known in the theory of elasticity as strain energy of the system.

Applying the first law of thermodynamics we find that

$$dU = dQ + \sigma d\epsilon \tag{3}$$

where:

dU= change in internal energy

dQ= change in thermal energy

σ = stress

$d\epsilon$= change in strain

For isothermal processes we can write:

$$d(U - E) = dQ \tag{4}$$

where:

U = internal energy.

E = strain energy.

Q = thermal energy.

This equation shows that the difference between internal energy and strain energy is exactly equal to the amount of heat which the system must exchange reversibly with the surroundings at temperature T. This energy is positive for materials with a positive thermal expansion coefficient, and opposite for materials with a negative thermal expansion coefficient.

The process of exchanging heat during reversible isothermal loading or unloading is referred to as the thermoelastic effect. Swalin[4] developed equation 5 to calculate temperature change due to the thermoelastic effect in tensile loading.

$$\ln\left(\frac{T + \Delta T}{T}\right) = - \frac{v\ \alpha \Delta\sigma}{3\ c_p} \qquad (5)$$

where:

ΔT= change of absolute temperature due to change in stress.

α = thermal expansion coefficient.

c_p= heat capacity at constant pressure.

v = molar volume.

$\Delta\sigma$= change in stress.

It is seen from this equation 5 that tensile stress causes the temperature of metal to decrease. Calculations(Appendix A) for steel show that the temperature

change due to the thermoelastic effect produced by a stress level of 500 MPa is equal to -0.16 K. The change in potential related to such change in temperature will depend upon the thermal emf coefficient. For steel it is ~1mV/degree[5]. So, the assumption in thermodynamic calculations of potential change due to stress that the process is isothermal and reversible doesn't cause a major error. Change in thermodynamic potential caused by strain energy and strain energy itself should be almost identical.

The most detailed thermodynamic analysis of the effect of stress on electrochemical potential of the metal was given by Flood[4]. He considered dissolution and deposition as essentially displacement processes. Such displacement potentials of the mass appearing in one state and disappearing in another should be equal at equilibrium. He arrived at the following equation 6 for the difference between reversible potentials of stressed and unstressed metal.

$$\Delta E = -\frac{1}{nF} \int_{\bar{p}_o}^{\bar{p}} V d\bar{p} - \int_{q_o}^{q} \phi dq \qquad (6)$$

where:

ΔE = difference of potential.

F = the Faraday constant.

n = valence of the ion.

$\bar{p}$ = final stress on the metal electrode.

$\bar{p_o}$ = initial stress on the metal.

V = electrode volume.

ϕ = plastic strain energy.

q = final strain energy on the metal electrode.

q_o= initial strain energy on the metal electrode.

$\bar{p} = \frac{1}{3}(px + py + pz)$

where:

px,py,pz = principal stresses in x,y,z directions.

Thus the displacement work makes the electrode more noble when the sum of the pressures or stresses is negative. Beyond the elastic limit shear strain energy is involved which always makes the electrode less noble. However, Flood says that the magnitude of shear energy cannot be calculated in a simple way. This equation holds for small px,py,pz changes below the elastic limit and for homogeneous materials so all parts of the system are in equilibrium, including the surface layer.

He also made the following remarks:

- If the surface of the electrode which controls the ionic equilibrium consists largely of detached particles of the metal so that less stress is sustained by the surface than applied the observed ΔE will be less than calculated.
- If the outer layer is work hardened it may sustain more stress and the measured ΔE will be greater than that calculated from equation 6.

Huffstutler' showed that the effect of elastic strain upon a single electrode potential expressed in

electrochemical terms theoretically for common metals was in the order of 0.0145 to 0.145 μV per 10MPa in the active direction.

Walker and Dill[9] showed by theoretical calculations that iron stretched to its elastic limit should produce an active shift in potential by 1.34 μV which is equal to 0.115 μV per 10MPa. A positive slope for an active shift refers to an old convention in which oxidation potential was used to rank metals in the electrochemical series.

2.1.2 Plastic strain effect.

According to Murata and Staehle[9] plastically strained electrodes are classified in two different categories:

1. cold-worked electrodes.
2. dynamically straining electrodes sometimes called straining electrodes.

The first category of deformation gives a permament shift in potential of the electrode. Graphical interpretation for expressing the manner in which cold working can affect corrosion potential and current was introduced by Evans in 1929, and explained in a paper published by Simnad and Evans'[10]. He said that corrosion potential change had little relation with reversible potential change. As the result of cold work, corrosion current will always increase while corrosion potential can change positively or negatively and equilibrium potential

changes to more active or remains unchanged.

The change in internal energy accompanying the cold working is the difference between work done during deformation and the amount of heat evolved. This energy was called by Taylor et al.[11] the latent stored energy. The authors mentioned the work done by Farren and Taylor which showed that this energy is equal only 5.5 to 13.5% of the total plastic work done. The magnitude of such energy can be calculated from formula 7 given by Bohnenblust and Duwez[12].

$$c = x_1\sigma(x_1) - \int_0^{x_1} \sigma(x)dx - \frac{1}{2}\, y\sigma(x_1) \qquad (7)$$

where:

c = latent energy caused by cold working.

x_1= tensile strain.

$\sigma(x_1)$=tensile stress at strain x_1.

y = elastic strain at stress $\sigma(x_1)$.

$\sigma(x)$= stress function of strain.

Hoar[13] showed thermodynamically that the maximum mechanical energy that can exist in a stressed metal or be stored in cold-worked metal is equivalent to a debasement of the reversible potential by only a millivolt or so.

The straining electrode gives a so-called transient potential change: it assumes a maximum peak value and decays gradually with time after loading is stopped. The transient

peak value always deviates in the more active direction and can reach the magnitude of hundreds of millivolts. This indicates that the transient potential is largely affected not by deformation energy but by deformation processes such as: breaking of film and formation of slip steps and kinks.

According to Howard and Pyle's[14] analysis, atoms at the edge of an infinite plane surface are able to dissolve at rates 10^4 times faster than atoms from the plane surface.

Hurlen[15] stated that transient behaviour is the indication that the dissolution and deposition reactions and surface properties are mutually dependent. This is based on the theory of crystal growth and dissolution[16,17,18]. This theory, developed and proved by many authors, says that at solid/solid ion solution equilibrium there is a continuous change of metal surface by flow of steps and kinks and other imperfections which are the lattice building and demolition sites.

Windfeldt[19] also believes that increased reactivity of the surface of deformed metal is due to an increased number of reaction sites in the surface of the yielding metal. The treatment which led him to develop an equation for peak potential in a straining electrode at constant current was based on a model which implies that the rate of dissolution and deposition of solid metal is proportional to both the kink density in steps and to the step density on the metal surface.

When it is assumed that the variation of the kink density in steps with potential is included in the exponential term by the Tafel slope value (b) the equation for a dissolution reaction obeying the Tafel law is

$$\frac{i'}{i} = \frac{s'}{s} \exp\left(\frac{V' - V}{b}\right) \tag{8}$$

where:

b = the Tafel slope value.

i'= dissolution rate at potential V'.

i = dissolution rate at potential V.

s = density of self-perpetuating steps.

s'= density of steps generated by the slip.

The density of self-perpetuating steps under steady-state conditions is proportional to the activation overvoltage given by equation 9.

$$s = k(V - E) \tag{9}$$

where:

k = nucleation constant.

(V-E)= activation overvoltage.

The total step density in the surface of a simultaneously yielding and dissolving metal under steady-state conditions can be given by equation 10.

$$s' = k(V' - E') + k'\frac{r}{i} \qquad (10)$$

where:

k'= a constant.

r = strain rate.

i = dissolution rate(constant).

This equation covers purely energetic and kinetic effects. It describes the effect of deformation processes occurring at a certain strain rate. When it is assumed that the energetic effect of strain is negligible (i.e., E'=E) and strain does not directly affect the kink density in steps, equations 8-10 give the following expression for the maximum potential change $\Delta V=V'-V$ when going from a strain-free to strain-dependent steady state under galvanostatic conditions (i.e., i'=i).

$$\Delta V = -b\ln(1 + \frac{\Delta V}{V - E} + \frac{k'r}{k(V - E)i}) \qquad (11a)$$

With an increasing strain rate to current ratio the equation can be written

$$\Delta V = -b\ln(\frac{k'r}{k(V - E)i}) \qquad (11b)$$

Equations 11 apply to dissolution and show that the maximum potential change accompanying plastic flow is negative. Equations 11 hold for straining in acid solution

where only activation polarization persists. If oxygen supply determines corrosion rate the equations are not obeyed.

An attempt at theoretical treatment of transient potential based on the film rupture model was made by Funk et al.[20,21] and Giddings et al.[22]. They state that the strain transient is a measure of the protective nature of the film. If the nature of the film is changed by changing content of the solution the strain transient is altered. According to their theory at the corrosion potential the film is formed and its nature depends on the oxidation power of the solution. When an electrode is plastically strained the brittle film is presumably ruptured exposing bare or near bare metal surface. This is tantamount to the destruction of the diffusion barriers in the ruptured region so that a different anodic reaction equilibrates rapidly. The new so-called steady state potential lies closer to the equilibrium potential of the metal. An exposed metal surface is short lived since reoxidation proceeds rapidly. Thus the steady state potential will decay back to its initial corrosion potential. This maximum voltage change is slightly less due to capacitance lag. Funk et al. called this property of strain electrochemistry the anodic potential transient. The typical potential strain curve presented in Figure 1 may conveniently be described in terms of three parameters:

- the maximum voltage.

- the elapsed time between the application of strain and the maximum voltage(growth time).
- the time in which potential decays from its maximum to one half of it (decay time).

An equation which approximates this voltage change with time is

$$\frac{d(CV)}{dt} = e\Sigma z_i[v_{io} \exp(\frac{z_i\alpha_i eV}{zkT}) - v_{io}' \exp(\frac{-z_i(1 - \alpha_i)eV}{zkT})] \quad (12)$$

where:

V = potential difference between electrode and solution.

C = the capacitance of unit area.

e = electron charge.

z_i= number of electron charges transported by a single i-th process.

α_i =fraction representing the free energy change due to potential, usually $\alpha = \frac{1}{2}$

v_{io}=anodic reaction velocity at initial state without strain.

v_{io}'=cathodic reaction velocity at initial state without strain.

k = the Boltzman constant.

T = absolute temperature.

Initially before the electrode is strained the potential is stationary so the left side of equation 12 equals zero. In the particular case in which z_i's are equal and α_i is equal

to 1/2:

$$V_{initial} = \frac{kT}{ze} \ln \frac{\Sigma v_{io}'}{\Sigma v_{io}} \qquad (13)$$

The point of the maximum change from the initial potential is also stationary with respect to potential and can be treated the same

$$V_{maximum} = \frac{kT}{ze} \ln \frac{\Sigma u_{io}'}{\Sigma u_{io}} \qquad (14)$$

where:

$V_{maximum}$= maximum potential of strained electrode.

u_{io}'=cathodic reaction velocity of strained electrode.

u_{io}= anodic reaction velocity of strained electrode.

The difference between the initial and the maximum potential is the result of the altered reaction velocities. The maximum potential change or the amplitude of the transient ΔV_m is found to be

$$\Delta V_m = \frac{kT}{ze} \ln \frac{\Sigma u_{io}' \Sigma v_{io}}{\Sigma v_{io}' \Sigma u_{io}} \qquad (15)$$

Next, the following assumption is made that the cathodic reaction velocity is not changed as the electrode is

strained,

$$u_{io}' = v_{io}' \tag{16}$$

and the anodic reaction velocity is increased proportionally to the relative elongation of the electrode s:

$$\Sigma u_{io} = \Sigma v_{io} + gs \tag{17}$$

where:

g= the relative anodic reaction rate of the clean metal surface (increases with order of metal in emf series).

When equations 16 and 17 are substituted in equation 15 we obtain

$$-\Delta Vm = \frac{kT}{ze} \ln(1 + \alpha s) \tag{18}$$

where:

$$\alpha = \frac{q}{\Sigma v_{io}} \tag{18a}$$

The value of α is dependent on the nature of the metal (g) and the oxide film. The authors found that the values of α increase in the order of the metal in the emf series except for Zn and Fe.

2.2 Literature review on the effect of stress, cold work and continuous straining upon potential of metal

2.2.1 Effect of stress

In 1907 Walker and Dill[4] wrote,

> "The condition which is supposed to influence the electromotive force of iron is the effect of stress upon the metal."

They reviewed some works in this field done by Wood, Andrews, Hambuechen, Richards and Behr, and found that the literature on this subject up to that date was quite inconsistent.

The authors themselves undertook an investigation in order to put some more light upon the question of sign and magnitude of the potential change caused by straining of pure iron below its elastic limit. The iron was smoothed with a file and medium emery cloth and put into an air-sealed ferrous sulphate electrolyte. The experiment on iron under continuous straining produced a potential change between 0.1 and 0.4 mV in the more noble direction. The same experiment in ferric chloride gave a potential change of 0.6 mV in the same direction.

Later, in 1946 Evans and Simnad[23] while doing corrosion fatigue tests on mild steel in 0.1N KCl, measured the potential change with elastic tensile and compression

stress. Specimens polished with emery paper and degreased with acetone were bent statically in the form of an arc. When the outer arc was exposed to the solution the specimen was in tension, and potential changed to a more anodic value; when the inner arc area was exposed the specimen was in compression and the potential changed to more noble with respect to unstressed metal.

In 1962 Tan and Nobe[24] tested annealed iron, cleaned with abrasive and etched in dilute HNO_3, in air saturated 1N $FeSO_4$ solution. The stress was applied statically by adding weights. They found a linear reversible cathodic potential shift with the slope equal to 18μV per 10MPa. They mentioned the work done by Giulotto in 1936 on iron in 0.05N $FeSO_4$ who found a similar linear positive potential change with a slope of 12μV per 10MPa.

Nonferrous metals have also been tested. Fryxell and Nachtrieb[25] investigated the potential of silver abraded and cleaned with 0.1N HNO_3 in 0.1N $AgNO_3$ solution. They found that tension produced a linear shift of potential in the cathodic direction with a slope of 0.113±0.021 mV per 10MPa. The effect was the same for stress applied by adding weights gradually. They also found that surface roughness influenced the compression potential coefficient of silver. An electropolished smooth surface produced a larger potential coefficient than a rougher surface obtained by mechanical grinding or fine machining.

Tan and Nobe[24] observed the slope of 0.1 mV/10MPa for silver in 1N silver nitrate solution with tension. The slope slightly increased in more dilute $AgNO_3$.

Nobe and Seyer[24] tested electropolished hard drawn copper in 1M NaCl solution by measuring potential with torsional stress. Their experimental results showed that the electrode potential within the elastic limit varied as the square power of the applied torque and the change was in the anodic direction.

2.2.2 Effect of cold work

Walker and Dill[9] also tested the potential between plastically deformed and annealed pieces of iron in ferric chloride solution. The test results showed that the cold strained piece was slightly more positive than the annealed.

Simnad and Evans'[10] examined the corrosion potential and depolarization effects of cold rolled steel and iron in 0.1N HCl oxygenated and deoxygenated solutions. Specimens were anodically etched free from pits and scratches. They found that the freely corroding potential of cold-rolled pure iron was a little more noble than that of annealed. The freely corroding potential of cold-rolled steel was slightly more anodic than that for annealed.

Anodic depolarization curves for iron and steel were shifted about 25 mV below their respective curves for annealed specimens. The cathodic polarization curve for cold-rolled iron was less steep than that for annealed iron.

Evans and Simnad[23] found that for mild steel the effect of cold working on potential in salt solution was negligible but if the test was done in acid solution the change reached 40 mV in the electronegative direction. They said that in acid solution where no film was present the potential change reflects the corrodibility of a distorted crystal structure.

Contrary to these results Foroulis and Uhlig[27] found a cathodic shift of potential for mild steel in 0.12N HCl pH 1.01 with cold work.

Salvago, Fumagalli and Sinigaglia[28] investigated the influence of cold working on the anodic behaviour of 304 stainless steel in 0.1N HCl at room temperature. They found that cold work lowered the critical pitting potential.

2.2.3 Effect of continuous straining

Walker and Dill[8] strained pure iron beyond the elastic limit in ferrous sulphate solution. They discovered that the potential suddenly changed in the active direction by several hundredths of a volt and the change ceased abruptly when straining was discontinued. The magnitude of the change depended on the strain rate. The same specimen under torsional stress gave results similar to those obtained from tension tests. When specimens were strained to their breaking limit the potential reached a constant value shortly after fracture. The difference between the initial and final potentials varied from -1.9 to 7.7 mV.

Windfeldt[19] tested the effect of plastic flow on electrode potential of iron in 0.01M HCl solution exposed to air under galvanostatic conditions. The strain was applied until fracture where the total elongation was 15%. He found that the potential changed immediately in the negative direction when plastic flow occurred. The rate of change was relatively high at first, then slowed down and the maximum change was usually reached after about two thirds of the flow period. After fracture the potential rapidly returned to nearly its initial value. The maximum potential change was between 5 and 20 mV with strain rate between 0.1 and 3%/s.

Stüwe and Pink[21] tested the potential change of steel in 0.1N NaOH solution with strain at various rates. The total applied strain for each specimen was 5%. They found the potential change varied with the power of strain rate.

$$U \propto \dot{\epsilon}^{\alpha} \tag{19}$$

where:

U= potential change for 5% strain.

$\dot{\epsilon}$= strain rate (s^{-1}).

α= equal to 0.5 for the tested steel.

Giddings et al.[22] recorded the strain transients of Cu, Al, Zn, Ni, Ag and Fe in distilled water at 25°C when strain ranged from 0 to 7%. They found that the transients depended

on the position of the electrode in the emf series. The transient peak value increased as the metal became more electronegative except for Ni and Fe. The plot of ΔVm vs. emf gave a smooth line except for Ni and Fe which lay below the curve since the porous film reduced the observed magnitude of the transient. The transient potential also increased with the amount of strain as predicted theoretically by equation 18.

2.3 Proposed theories of stress and strain effects

2.3.1 Stress effect.

Summarizing the previous work the potential change in the elastic tension region was in the noble rather than in the active direction. The magnitude of the change was about 1 mV which is higher than predicted thermodynamically. The change was linear with stress and reversible. Authors agreed that the effect was not caused purely by stress. According to them some kind of surface phenomenon was responsible for this.

Burgess[30] explained it as an excessive storing of energy in the outer layer of metal.

Evans and Simnad[23] concluded that stressing within the elastic limit affects the potential by altering the state of repair of the film covering the surface.

Harwood[31] stated that in polycrystalline materials grains of different orientation take up different degrees of stress. Presumably a small amount of slip in favorably oriented grains can be the cause of the change.

However, this seems unlikely because slip would more likely break the film which in turn would be manifested by transient behaviour. Although in work done by Tan and Nobe[23] on brass in copper sulphate solution such transiency was observed, it was explained by theoretical consideration of the double layer.

Harwood[21] also reasoned that the degree of orientation dissimilarity at grain boundaries produces some stress. Under external load this stress is magnified in various ways.

Fryxell and Nachtrieb[22] wrote that the thin oxide film on the surface may become distorted or disrupted under elastic stress. If the film is distorted it offers a different barrier for the electrode reaction. However, they added that attempts to test this hypothesis have yielded negative results.

The same authors tried to assess the role of dissolved gasses such as used in deaeration and found that the tension coefficient was independent of the nature of the gas including oxygen. Further they demonstrated that the nature of the surface was the contributory factor in potential change. They found that silver in compression showed a larger change of potential when the surface was electropolished than when the surface was prepared by mechanical ways. They suggested that rough surfaces concentrate stresses in peaks and valleys which results in nonhomogeneous distribution of energy.

They also considered the possibility of affecting the emf by the concentration gradient of ions ejected into the solution when stress is applied. This effect should be changing with time due to diffusion and could be reduced by agitation of the solution.

Simnad and Evans'[8] said that mechanical surface preparation can introduce stresses to the surface layer of annealed specimens and can mask true stresses of a cold-worked structure.

Simnad[32] reviewed a number of investigations on deformed surface layers with X-ray techniques. According to some data the mechanical polishing can produce distortion of the surface layer down to 25 μm in the case of steel.

While the magnitude of potential change with stress found a large number of theoretical bases the direction of the change did not draw as much attention among researchers. Theoretical considerations overwhelmingly agree that any increase of energy of the metal such as by application of stress must produce the potential change in the more active direction. Only Flood[4] in his thermodynamical consideration showed that a noble change of the potential should accompany compression.

Because of some inconsistency of the results and lack of interpretation of a noble change of potential in elastic tension, there is still a need to do more precise measurements to avoid masking the results by external factors.

2.3.2 Cold work effect.

Strain energy produces much higher effects than stress, but several different cases must be distinguished.

- Corrosion potential in film forming systems is not

affected appreciably by cold-work.

- Polarized potential in acid solutions where no film can survive changes in an unpredicted way, always leading to increased dissolution rate.

Evans(explained in reference 10) gave the first graphical explanation of such unpredicted behaviour. According to this interpretation strain energy can reduce the cathodic polarization and shift the whole anodic polarization curve down in a more active direction. As the result of such effects the overall corrosion potential can be shifted to a more noble value. The equilibrium potential (determined by taking a depolarization curve) changes in the more active direction which is in accordance with thermodynamic predictions. The magnitude of the change cannot be explained on simple thermodynamic bases. The calculated potential value is an average one for pure metal and can be altered when latent energy is not uniformly distributed or the metal is impure.

In Simnad's review[32], work done by Wood with the aid of X-ray techniques proved that about 5% of the cold-worked surface contains strain energy 500% higher than that in homogeneous places. Impurity segregation at imperfections (Cottrell atmospheres) establishes a galvanic cell.

Foroulis and Uhlig[27] wrote:

"the effect of cold-work on corrosion of metals in general is greatest when a second phase precipitates to form active galvanic cells, whereas the increase in

internal energy of a disarrayed metal lattice has little if any effect."

They found that dislocations carrying carbon reduce hydrogen overvoltage.

Texture produced by cold work is a significant factor in the electrochemical behaviour of metal. Harwood[31] reviewed some works on investigation of the crystal orientation effect on potential. According to figures shown in this review the (111) face in a single aluminum crystal is about 50mV more negative than the (001) plane.

Foroulis and Uhlig[27] say that preferred orientation of surface metal resulting from cold work may either increase or decrease corrosion depending on the orientation developed.

Precipitation of a second phase and phase transformation caused by cold work as indicated by Harwood[30] render metal susceptible to localized corrosion.

Huffstutler[7] explained the effect of grain boundary areas, which in certain alloys are present with higher dislocation density, as a tendency to segregate solute and impurity elements or massive precipitation of intermetallic compounds. The areas accommodating all these are more active than grains themselves.

2.3.3 Straining electrode effect.

A metal electrode in aqueous solutions acquires a potential as a result of electrochemical reaction near the metal/solution interface. When the electrode is strained the electrochemical barriers and reaction rates change causing the potential to change. The character of the change is transient and the peak value ΔVm which is used as a measure of such change is high, ranging from several mV to several hundreds mV in the more active direction. The value of ΔVm depends on the metal, solution, amount of strain and strain rate.

Walker and Dill[8] considered first the temperature as the probable cause. Their experiment showed that the temperature of the stretching specimen rose considerably with elongation. They examined the temperature coefficient for potential and found it was positive. Because of that the specimen should cool off on stretching which is opposite to physical proof from experiment.

Windfeldt[10] proved that the maximum transient potential generated in acid solution was proportional to both the kink density in steps and to the step density on the surface in a yielding material. He also found that the change of potential due to applied strain was independent of pH which was contradictory to what Giddings[22] et al. tried to assess.

Hurlen[5] stated that the question remained whether potential change increase with strain rate was due to speed of forming steps or other causes.

Giddings et al.[23] said that the magnitude of the strain transient for a metal was related to the chemical and physical nature of the protective film along with the position of the electrode in the emf series. They also proved that ΔVm increased with the amount of strain applied according to their theoretical equation. In this theory it was assumed that anodic reaction velocity increases due to increase of anodic area caused by film break.

Hurlen'[5] explained that the increase in anodic area with deformation was caused by formation of slip steps on the surface of the deforming specimen.

Consequently, it seems safe to suppose that the value of peak voltage generated in a straining electrode is the result of both break of film and formation of slip steps.

3. EFFECT OF VELOCITY OF FLOW ON ELECTRODE POTENTIAL

3.1 Theory

Fontana and Greene[1] described the effect of velocity as complex and dependent on the characteristics of the metal and environment to which it is exposed. The effect basically can be of three different types:

1. For corrosion processes which are controlled by activation polarization, velocity has no effect.
2. If the corrosion process is under cathodic diffusion control the velocity:
   a. increases the corrosion rate in the active potential region. This effect generally occurs when an oxidizer is present in very small amount as in the case for dissolved oxygen in acid or water.
   b. has no effect if the metal is readily passivated.
3. For some metals forming massive bulk visible films of corrosion products, velocity has virtually negligible effect until the damage or removal of such scale occurs.
   When scale is removed it results in accelerated attack and the process is known as erosion-corrosion.

The effect described in (2.a) occurs when the supply of reactant to the reaction surface or removal of reaction products from the reaction surface is controlled by diffusion. Usually the corrosion process is limited by supply of reactant to the reaction surface. This effect is demonstrated in figure 2 taken from Fontana and Greene[32]. Corrosion current density controlled by diffusion is called limited current density (LCD). Supply of reactant to the reaction surface in a stagnant solution is governed by molecular diffusion and is slow. Once the solution is stirred, convective diffusion begins to dominate and LCD increases.

Levich in his book[34] explains in detail the role of hydrodynamics on electrochemical processes. If it is assumed that the solution is an incompressible liquid and the diffusion coefficient is independent of concentration of the solute, the equation for mass flux of particles to the reaction surface can be written

$$j = D \frac{c_o}{\delta} \qquad (20)$$

where:

j= flux of particles.

D= diffusion coefficient.

c_o= concentration of the particles in the bulk.

δ= thickness of diffusion layer.

LCD resulting from mass flux is expressed by the equation:

$$LCD = n\ F\ D\ \frac{C_o}{\delta} \qquad (21$$

where:

n= valence of dissolving ion.

F= the Faraday constant.

The magnitude of polarization caused by diffusivity and concentration gradient called concentration polarization can be written:

$$\eta_c = \frac{RT}{nF} \ln\left(1 - \frac{i}{i_L}\right) \qquad (22)$$

where:

η_c= concentration polarization.

R= the Boltzman gas constant.

T= absolute temperature.

i= net current flow.

i_L=limiting current density.

The diffusivity and concentration gradient depend on the flow regime which can be: laminar, transition or turbulent. These regimes are defined by a dimensionless number called the Reynolds number (Re) which is the function of the following:

$$Re = f(\upsilon, d, \nu, h, g) \qquad (23)$$

where:

υ= mean velocity of the stream.

d= characteristic dimension of the stream section.

ν= kinematic viscosity.

h= roughness of the solid surface.

g= geometry of the stream.

In laminar established flow the viscosity between layers of the stream and the stream with the solid wall due to molecular cohesion plays a dominant role. In this region the convective diffusion coefficient remains constant; however LCD will increase with velocity due to decrease in thickness of the diffusion layer.

In the transition region, collision between molecules and molecules with the solid wall begin to predominate and affect viscosity. Producing this so-called eddy viscosity improves diffusivity and thus LCD.

In the fully developed turbulent region the thickness of the diffusion layer is assumed to be constant but an increasing scale of turbulence with velocity will still affect diffusivity and increase LCD.

Poulson[38] gives the procedure to correlate LCD with velocity of flow. In this approach the mass transfer coefficient defined as overall transport to the surface based on laminar and turbulent convection was introduced.

$$K = \frac{\text{rate of reactivity}}{\text{concentration driving force}} \qquad (24)$$

Reaction rate involving the coefficient K for a diffusion controlled system can be expressed:

$$LCD = K\ n\ F\ \Delta c \qquad (25)$$

where:

K= mass transfer coefficient.

Δc=concentration difference.

The coefficient K is incorporated in a dimensionless number called the Sherwood number according to the following relation:

$$Sh = \frac{K\ D}{d} \qquad (26)$$

where:

Sh= the Sherwood number.

K = mass transfer coefficient.

d = characteristic dimension of stream cross section.

D = diffusion coefficient.

The Sherwood number in turn is a function of the Reynolds number and Schmidt number (Sc). Such relationships are usually obtained as empirical correlations of experimental data for a certain flow geometry and regime.

They are usually of the form

$$Sh = \text{constant } Re^{x} Sc^{y} \tag{27}$$

where for tubular geometry with a smooth surface:

$$Re = \frac{v\ d}{\nu} \tag{28}$$

$$Sc = \frac{\nu}{D} \tag{29}$$

where:

Sc= the Schmidt number.

d = diameter of the pipe

x = usually between 0.3 and 1.

y = typically 0.33.

The effect described by Fontana in point (3) is the effect of momentum transfer between the fluid and solid wall. The resultant force called the drag force produces shear stress between solid surface particles and fluid molecules called wall shear stress. The magnitude of such stress is a function of Re and the surface roughness.

Vennard and Street[36] give the theoretical treatment of such effects. They say that flow is always affected to some extent by the solid boundary over which it passes. For a

real fluid experimental evidence shows that the velocity of the layer probably having a thickness of a few molecules adjacent to the surface is zero. In laminar flow the velocity profile is parabolic and the shear stress profile is a straight line with the largest value at the boundary. In this regime viscous effects dominate the whole flow and the surface roughness has no effect on the flow picture as long as the roughness projections are small relative to the flow stream cross section. The wall shear stress in this region is dependent only on Reynolds Number (Re).

In the turbulent flow regime logarithmic velocity profile is applicable. In this regime there is a continuous mixing process of eddy velocities with viscous stream lines across the stream. The turbulence is completely extinguished in a region very close to the boundary and a film of viscous flow called viscous sublayer results over the boundary. In smooth pipes shear stress is proportional only to the Reynolds number (Re).

In rough pipes, roughness will change the size of the viscous sublayer and thereby affect the character of the flow and the friction factor. The effect of roughness is complex and depends on the size of the roughness relative to the thickness of the viscous sublayer.

Experiments have shown that roughness heights larger than about one-third of the viscous sublayer thickness will augment the turbulence. Roughness heights 6 times larger than the sublayer thickness will change the flow to

completely turbulent.

The wall shear stress in rough pipes will depend on both the Reynolds number and the relative size of the roughness and thickness of the viscous sublayer. Both variables increase with velocity of flow. In other words, pipes that are smooth at low values of the Reynolds number become rough at high values of Re. This is explained by the thickness of the viscous sublayer which is decreasing as the Reynolds number increases, thus exposing smaller roughness perturberances to the turbulent regime and causing the pipe to exhibit the properties of a rough one.

3.2 Literature review

Ross and Hitchen[37] tested the effect of flow of oxygenated water upon the electrochemical behaviour of tubular couples of iron and copper, carbon and copper, and copper tubes of different diameters. The electrochemical behaviour was examined by measuring anodic and cathodic polarization characteristics at flow rates ranging from laminar to turbulent.

The iron-copper couple was assembled by fixing an iron rod centrally in the copper tube. Potential and current measurements were recorded when steady readings were obtained. Their results showed that anodic polarization behaviour of steel was little affected by flow rate but the copper cathode was rendered more noble and less polarized at increased flow rate. The couple potential shifts in the

noble direction and increase of corrosion current were more pronounced in the laminar regime than at higher flow rates. The authors said that the results illustrated clearly the importance of the fluid velocity effect on a cathodic process controlled by the rate at which dissolved oxygen is made available at the cathode surface. According to the known relationship the rate is proportional to bulk concentration and inversely proportional to the thickness of the diffusion layer.

They explained that under laminar conditions the thickness of the diffusion boundary layer is large; therefore the cathodic depolarization and corrosion potential are sensitive to the Reynolds number. Under turbulent flow conditions the thickness of the diffusion boundary layer changes much less than in the laminar regime; therefore cathodic depolarization and corrosion potential may be relatively insensitive to Reynolds number.

The slight effect of flow rate over a large range of Re on the iron anode was explained by the argument that states that the rate of formation of ferrous ions at the iron surface always exceeds or equals the rate at which they are transported by diffusion and turbulence.

When the iron rod was replaced by a carbon rod, copper became the anode. The results of this couple showed that in the laminar regime copper became less polarized and its corrosion potential changed to less positive, but on transition to turbulence the anode became ennobled although

depolarization continued. The carbon cathode became more noble and less polarized with increasing flow rate. In their interpretation, the falling slope of the anode polarization with inceasing flow rate was due to lower ability of copper to form ions in neutral aqueous solution so that the rate of dissipation of copper ions from the surface exceeded the rate of their formation. The ennobling tendency of the copper-carbon couple potential in the turbulent range was explained by the effect of passivation of the copper surface by transferring oxygen at a higher rate.

They also demonstrated the flow rate differential potential for copper by forcing liquid at different rates through two copper pipes of different size. They found that in the turbulent regime the smaller diameter tube became the anode with respect to its larger diameter partner. At a lower flow rate, such that laminar flow existed in the larger tube and turbulence developed in the smaller, the latter became the cathode.

To explain this they examined the polarization characteristics of a single copper tube at different velocities of flow. Polarization diagrams showed that the corrosion potential of copper fell with velocity of flow in both laminar and turbulent regimes, but it sharply increased on transition. The anodic Tafel slope was decreased in both laminar and turbulent regimes although it changed oppositely on transition.

Further, they also observed a temporary reversal of polarity

subsequent to a sudden change in flow rate. At zero flow rate the two tubes showed almost the same potential, but after suddenly established turbulent flow the smaller diameter tube developed a cathodic property which persisted for about 20 minutes. At that time it reverted to its anodic position; repetition of this cycle at the same and other flow rates proved similar behaviour. They explained that the delay of the surface exposed to the lower velocity in attaining equilibrium was attributed to the lower rate of filling the boundary layer with oxygen by diffusion when the boundary layer underwent a transitory effect because of changed concentration gradient.

Mahato et al.[38] in their work tested the electrochemical behaviour of 6 inch and 12.75 inch diameter black iron pipes in city tap water at a velocity range equivalent to Reynolds numbers 6500-39320. They found that the corrosion potential changed to more noble and the corrosion rate increased with velocity of flow. They also observed that for fixed velocity the corrosion rate fell rapidly with time before it stabilized gradually at a more or less constant level while the corrosion potential first suddenly fell and then gradually increased to a stable value. The authors explained this behaviour by considering the effect of velocity on the mass transfer rate.

Lee et al.[39] examined the effect of flow rate on corrosion potentials of 15 materials in sea water at 10 to 25°C. Their results showed that for carbon steel, increasing

velocity of flow changed the corrosion potential in the more noble direction at both temperatures; however the corrosion potential shifted in the active direction with an increase in temperature.

4. EXPERIMENT, RESULTS AND CONCLUSIONS

4.1 Material, solution and initial measurements

4.1.1 Material.

Plain carbon steel in the as-received condition was used.

The chemical composition of the material was analyzed with an Atomic Absorption Perkin-Elmer model 4000 Spectrometer and LECO carbon/sulpher analyzer.

The results of the analysis in weight percent are given in Table 1.

Table 1. Chemical composition of the test steel.

C	Mn	Si	S	Cr	Ni	Mo	Al	Pb
0.24	0.59	0.01	0.04	0.149	0.189	0.049	0.099	0.039

Mechanical properties were determined by doing a tensile test on a round specimen. The specimen was machined to a diameter of 0.5 inch and gauge length of 2 inches. The other dimensions of the specimen were different from that given by ASTM A370-87a standards. The test was done mainly in order to measure the yield strength of the test steel because part of the experimental tests were to be done below the yield

point. The tensile test results are given in Table 2.

Table 2. Mechanical properties of the test steel.

Yield Strength MPa	Tensile Strength MPa	Elongation %
452.9	467.2	19.0

4.1.2 Solution

Three percent NaCl in deaerated distilled water solution was used.

Deaeration was done by bubbling nitrogen gas through the solution until a constant reading close to zero on the galvanic cell oxygen analyzer type GCA/Precision Scientific was obtained. The reading remained constant during the test. The temperature of the solution was kept between 24 and 25°C for all velocity ranges except for stagnant conditions where temperature equalled the room temperature, that is 22.5°C. The temperature variation during the test at each velocity of flow was less than than 0.2°C.

The pH of the solution was 7.4 and it changed slightly to higher values with the duration of the test. The viscosity of the solution, determined with a Brookfield viscometer was 1.1×10^{-3} Pa·s. The density of the solution ρ = 1007kg·m^{-3}.

4.1.3 Corrodibility of the steel in the stagnant solution.

The corrodibility characteristics were obtained by taking anodic and cathodic polarization curves according to the requirements of the ASTM G5[40] standards.

The following instruments were used:

- testing cell.
- saturated calomel reference electrode.
- Pt counter electrode.
- ECO Model 551 Potentiostat-Galvanostat.
- ECO Model 567 Digital Function Generator.
- ECO Model 560/LOG Linear/Logarithmic Interface.
- Hewlett-Packard Model 7044A x-y recorder.

Tests were repeated until good reproducibility was obtained. The polarization curves are presented in Figure 3. It can be seen from the diagram that polarized potential higher than the active region caused the corrosion rate to reduce slightly due to formation of corrosion product film on the surface of the metal. On cathodic polarization there is evidence of a concentration polarization effect due to the presence of a small amount of oxygen.

4.1.4 The quality of the film formed at a potential above the activation polarization range.

The quality of the film was examined with $CuK\alpha_1$ X-rays on a Rigaku-Denki Model D-F3 diffractometer. The results of the test are shown in Table 3. Based on the analysis of the diffraction patterns it was found that the film contained

mainly iron oxide hydrate $Fe_2O_3 \cdot H_2O$.

Table 3. The results of the X-ray data search.

No.	Θ degrees	d_{hkl} Å	$Fe_2O_3 \cdot H_2O$	Fe_2O_3
1	8.1	5.46	5.48	
2	8.35	5.30		
3	9.0	4.92		
4	11.4	3.90	3.65	3.73
5	13.85	3.22		3.41
6	14.85	3.00		2.95
7	15.95	2.80	2.75	2.78
8	17.15	2.61	2.66	2.64
9	17.65	2.54		2.52
10	18.1	2.48	2.46	2.41
11	18.8	2.39	2.20	2.32
12	21.65	2.087		2.08
13	23.75	1.912	1.93	
14	24.35	1.867		1.87
15	25.5	1.789	1.71	1.70
16	30.25	1.528	1.525	1.61
17	34.5	1.359		1.32

4.1.5 The microstructure of the test steel

The section for the test was taken from the axial section of the 1025 hot rolled steel rod. A small piece of

steel was mounted in Bakelite thermoset material and ground with SiC paper down to #600 grit size. Then, the specimen was polished with diamond paste of 6 micron and 0.05 micron alumina. The polished surface was etched with 1% nital until the microstructure was clear for microscopic examination. The photograph of microstructure was taken with a Polaroid camera mounted on a Zeiss Metallograph Microscope. Figure 4 shows the typical steel microstructure consisting of ferrite and pearlite.

4.1.6 Measurements of residual stresses in the surface layer

The specimen was cut out from the rod in the as-received condition along its axis. The surface condition was obtained by consecutive grinding with #120, #240, #320, and #400 SiC papers.

The state of the biaxial stresses in the plane of the ground surface was examined by measuring d_{211} in α Fe with the CoKα wavelength. The test was performed on an X-ray diffractometer TuR M62 in the Metallurgical Engineering Department at the University of Mining and Metallurgy in Cracow, Poland by Dr. Stanislaw Skrzypek. The analysis of the results showed that the surface layer was in compression and the magnitude of σx and σy was 270±10 MPa.

4.2 Program and procedure of the test.

4.2.1 Tests in elastic loading range.

The steady state corrosion potential change was measured with continuously applied uniaxial tensile stress on loading and unloading at the rate of 0.5 $mm \cdot min^{-1}$ up to 385 MPa for the following velocities of flow: 0.0, 0.1, 0.25, 0.5, 1.5, 2.5, and 3.5 $m \cdot s^{-1}$. Velocities of flow and corresponding Reynolds numbers calculated by equation 28 are in Table 4.

Table 4. Velocities of flow and corresponding Reynolds numbers.

v $m \cdot s^{-1}$	0.0	0.1	0.25	0.5	1.5	2.5	3.5
Re	0.0	1100	2750	5500	16500	27500	38500

4.2.2 Tests in plastic loading range.

The steady state corrosion potential change was measured with continuously applied strain at the rate of 0.5 $mm \cdot min^{-1}$ up to 0.3% of plastic strain past the yield stress and on unloading. Measurements were repeated for five consecutive loadings and unloadings with the same amount of plastic strain in each on the same specimen at constant velocity of flow.

This test procedure was followed with new specimens for each of the following velocities of flow: 0.0, 0.1, 0.5, and 1.5 $m \cdot s^{-1}$. These flow rates in smooth pipes correspond to the following flow regimes: stagnant, laminar, transition and turbulent.

4.2.3 Specimen preparation and instrumentation setup.

1. The specimen was machined from the steel rod to the desired dimensions shown on Figure 5. The inner surface of the hole was finished by grinding with #400 SiC paper. This operation, followed by washing with soap and rinsing with acetone, was repeated each time before taking measurements.
2. The corrosion cell was prepared by washer connections to flow lines as shown in Figure 6. The corrosion cell tightened in the grips was put in the Instron Tensile Machine, Floor Model TT-D.
3. The solution flow was commenced from a specially designed circulation system shown on Figure 7. The desired flow rate was controlled by a previously calibrated opening of the ball valve. The temperature of the solution was maintained by using a cooling coil inside a 22 litre tank. Slightly positive pressure inside the tank was maintained by bubbling with nitrogen at very low rate to avoid air being sucked in during circulation of solution.
4. The potential of the steel sample was measured vs. a

saturated calomel electrode. The measurements were recorded on Hewlett-Packard Model 70 44A x-y and Ricadenki Model 3-361 XA recorders hooked up with a high impedance differential amplifier and oscilloscope. Amplification of the output increased the precision of potential measurements to better than 0.01 mV. The oscilloscope was used to detect noises in the circuit coming from external electromagnetic fields.

4.2.4 Test procedure.

Once the corrosion cell and instrumentation were set up ready for the experiment, the test was performed by the following steps.

1. Commence solution flow at the desired rate.
2. Set up the appropriate cooling rate and monitor the potential development until the required stability is achieved.
3. Subtract the stable potential value with a differential amplifier.
4. Turn on the recorder and apply load.
5. Unload after a desired stress or strain level is achieved.

4.3 Results and discussion

First, to make sure that the net effects of stress and flowing liquid were examined, the stability of the potential of the unstressed specimen in stagnant solution was measured. Also the stability of the potential in stressed and unstressed conditions at a selected arbitrary velocity was recorded.

The results in Figures 8 and 9 show that steady state conditions were achieved for a period of about 2 min which is the time required for loading the specimen up to its yield stress at the designed rate. Fluctuations of the potential were minor, less than 0.05 mV and could not mask the real trend of stress and flow effects. Lack of transiency of the potential eliminates the influence of minor temperature changes due to stressing or flow friction. These conditions were obtained after a period of 3.5 to 4 hours between commencing of solution flow and application of load.

4.3.1 Results obtained from elastic loading

For each velocity of flow the corrosion potential at steady state conditions was noted and continuous curves of potential change with increasing stress (loading curves) and decreasing stress (unloading curves) were recorded. The unloading curves start from opposite sides on each diagram, which is a feature of the X-Y recorder used in the experiment. The stress axis refers to increasing stress

during loading and decreasing stress on unloading. At least two sets of curves for each flow rate were obtained to show that the results are reproducible. Copies of the chart records in reduced form are presented in Figures 11 to 17.

The way the corrosion potential changed with velocity of flow is shown on Figure 10, curve 1, and it can be described as follows:

The corrosion potential increased rapidly in the laminar flow regime and in the transition region. In the turbulent flow regime the increase of the corrosion potential decreased and seemed to level off at higher flow rates. This effect can be explained by an increasing flux of reactant to the surface of the dissolving metal as flow rate increases.

The mass transfer increased with velocity of flow due to the increase of concentration gradient and to a lesser extent the increase of diffusivity. As a result the limiting current density increased causing the potential to rise along the anodic Tafel slope. This assumption that velocity of flow affects only the cathodic reaction of oxygen is supported by some investigations reported in the literature[37] which proved that flow rate did not have any effect on anodic polarization of iron in distilled water.

From Figures 11 to 17, it can be seen that the stress shifted the steady state potential in the noble direction at each velocity of flow. The change was linear with increasing stress and reversible on unloading. In stagnant solution the corrosion potential changed by 0.67 mV when stressed up to

385 MPa which was equal to 1.74 μV/MPa. These results compare reasonably well with results obtained by other investigators for iron and steel in different solutions (the results are quoted in the passage on literature review). Theoretical calculations based on thermodynamics would predict an active shift of the potential with tensile stress. Walker and Dill[4] showed that for iron the shift should be equal to -0.115 μV/10MPa. Considering the tensile data for 1025 steel obtained in this work, the calculated slope(Appendix B) is -0.0346 μV/MPa.

These results show that strain energy affected the potential to a larger extent and in an opposite way to thermodynamic predictions. This behaviour was reported in many previous works and some theories proposed by the authors have been mentioned in this thesis in the section on proposed theories of elastic and plastic strain effects on potential of the metal.

Theoretically only Flood[4] predicted a noble shift of potential with stress, but for compression loading.

This thesis will first consider the theory that internal stresses in the surface layer produced by the mechanical method of sample preparation are responsible for such a contradictory effect. This ennobling effect of the strain energy suggests that during uniaxially applied stress there must be a continuous dissipation of energy. Because the electrochemical potential represents a property of the metal surface, the dissipation of energy on tension can only

occur when the surface stresses are compressive before the load is applied.

If this were true the potential should change its trend when the bulk stresses in tension exceed the magnitude of compressive stress existing in the surface layer. The change was expected to happen at a stress level of 270 MPa.

The results obtained in the present work did not show the expected changes, which would eliminate this model of explanation unless the magnitude of compressive stresses measured in a flat surface is much less than that existing in the inner cylindrical surface which was used in the experiment. Determination of internal stresses in an inner cylindrical surface is very difficult.

Another possible explanation might be that the distorted layer could dissolve during the period of waiting for the potential to stabilize. This, however, seems unlikely since the corrosion rate calculated for this corrosion cell(Appendix C) is equal to 0.241×10^{-3} μm/hour which is too slow to dissolve a surface layer 25 μm thick. This deformed layer thickness of 25 μm was determined by Vacher and quoted in Simnad's review[32].

On the other hand, if compressive stresses in the surface layer of the anode are not responsible for a noble shift of potential, the stress effect has to be explained by adopting Evans' graphical interpretation used for stress and cold work effects described in reference 10. According to this explanation one of the possible effects of stress on

corrosion potential is to reduce cathodic polarization and thereby shift the potential in the cathodic direction.

Figure 18 shows, as marked by the falling slope of straight lines, that the effect of stress on corrosion potential decreased with flow rate. The exact trend of the falling slope is shown in Figure 10, curve 2. It is quite noticeable that the effect of stress changes with velocity of flow in exactly the opposite way to the potential change. In other words, the effect of stress on the steady state potential decreases when oxidation power of the solution (corrosiveness) increases. This behaviour of the stress effect on potential with velocity of flow suggests that stress affects only anodic polarization of steel by decreasing it. Or, if the stress has a catalytic effect on the cathodic process, the effect may be reduced in flowing solution where the cathodic process is less diffusion controlled.

4.3.2 Results obtained from plastically straining electrode.

The results in the form of digitized copies of chart records are in figures 19 to 23. The set of four curves obtained at each velocity of flow during corresponding loading cycles are put on one diagram in order to show the effect of flow on the potential transient more clearly.

Generally the behaviour of corrosion potential with loading beyond the elastic limit can be described in the following way:

The corrosion potential rose linearly in the noble direction with loading up to the yield stress, then depending on the number of straining cycles and velocity of flow the corrosion potential changed in the plastic region as follows:

During the first straining by the amount of 0.3% plastic deformation, Figure 19, in stagnant solution, laminar and transition regimes the corrosion potential continued rising more sharply. The potential kept rising also on the unloading part of the cycle, and after reaching a maximum value it began to fall slowly with time. In the flow rate equivalent to a turbulent regime it shifted a little in the active direction. On unloading it rose sharply in the noble direction and after reaching a maximum value it began to fall slowly toward its original value.

During the second loading by an additional 0.3% plastic deformation, Figure 20, in stagnant solution and laminar flow it continued rising at a little higher rate than in elastic deformation and then on unloading it rose sharply. After achieving a maximum value it started to fall slowly with time to above the initial value.

At velocities corresponding to transition and turbulent flow the potential shifted in a more active direction reaching a negative peak value at the end of loading. On unloading the potential returned sharply in a more noble direction and after reaching a maximum value it started to fall slowly down to its initial value.

During the third straining cycle by another 0.35% plastic deformation, Figure 21, the potential shifted in the active direction in all stagnant and flowing solutions, reaching a negative peak value which was more negative at higher velocity.

On unloading the potential came back sharply to a more positive value and after reaching a maximum, began to fall slowly to a little above the original value.

During the fourth and fifth loading by another 0.3% and 0.35% of plastic deformation, Figures 22 and 23 respectively, it responded similarly to the behaviour observed in the third cycle; however the final potential values began to fall below their original levels.

The diagrams show clearly that the negative potential peak value became more negative with both increasing plastic deformation and velocity of flow except on the fifth straining cycle where the negative potential peak value in transition flow was more negative than in turbulent. This probably happened due to necking which gave more than the assumed amount of plastic deformation. The increase of the peak value with amount of deformation was reported by many previous investigators who explained it as due to the increase of slip step density and the anodic area.

The influence of velocity of flow on potential peak value, to this author's knowledge, has not been reported in the literature before. Thermodynamically such an effect would have to be related to some kind of additional energy

that atoms at the edge of newly protruding slip steps acquire during the flowing of liquid over them. This energy could be coming from two different sources: one from the viscous shear stress at the solid/liquid interface, and second from momentum transferred between moving solution molecules and the solid wall.

The diagrams also show two types of transiency: noble and active. In view of well established theory, which says that an active shift of potential occurs when fresh bare metal is exposed to a solution after film rupture, it can be easily seen from the results that different amounts of plastic deformation were required at different velocities of flow to expose bare metal. In stagnant solution and laminar flow regimes the film ruptured after application of 0.6% plastic deformation. In transition flow the film broke after only 0.3% plastic deformation was applied. In the turbulent regime bare metal was exposed on the first cycle of straining, that is, on the onset of plastic deformation.

Occurrence of this effect suggests that film quality changes somewhat with velocity of flow. In stagnant solution and laminar flow regimes the film seems to be more flexible than at a higher velocity range. This can be explained by considering the contribution of wall shear stress. As velocity increases the magnitude of wall shear stress increases, stressing the film to a larger extent so less applied strain would be required to break it. The ennobling transient which occurred under the condition where

presumably the corrosion film was stretched rather than broken is not fully understood. However the classic model of a catalytic role of a stressed crystal lattice for oxygen reduction could be adoptable.

The decay curves of the anodic transient changed with velocity of flow. As shown in Figure 24, the decay time to any arbitrarily selected potential level shortened as velocity of flow increased. The process responsible for the decay is widely recognized as a repassivation one. This process must be dependent on the oxygen supply rate since this rate, as it was explained earlier, increases with increasing velocity of flow.

It is very clear from these results and discussion that velocity of flow affects deformation processes which are responsible for environmental fracture. Straining cycles with a small amount of plastic deformation in each, which were made to imitate a fracture process gave unquestionably different potential records in different flow regimes. These effects, however, can only be considered with respect to the initiation stage of fracture which occurs at the surface of the metal over which 100% of the effect of the flowing stream applies. The velocity of flow effect on deformation processes occurring at the crack tip would have to be considered differently since hydrodynamics of the stream in a pipe are not related to hydrodynamics existing in a crack.

4.4 Conclusions

1. The results of the tests have shown that uniaxial tensile stresses shift the steady state corrosion potential of 1025 steel in 3% sodium chloride solution in the noble direction. The shift is linear and reversible on unloading. The results agree reasonably well with results of other investigators.
2. Increasing velocity of flow between 0 and 3.5 m/s increases the steady state corrosion potential from -779.5 mV to -740.0 mV (measured versus SCE) and reduces the effect of stress. The effect of uniaxial stress in the elastic strain region was reduced from 1.7 μV/MPa to less than 0.8 μV/MPa.
3. The results from the testing of plastically straining 1025 steel electrodes in the same solution have shown that increasing velocity of flow between 0 and 1.5 m/s increases the reactivity of the steel, increasing the negative peak value of the potential transient by about 2mV, approximately independent of the amount of plastic strain in the specimen.

   Ductility and reformation rate of the corrosion film are affected by velocity of flow. The film forming at higher velocity of flow needs less deformation to break and reforms faster.

Conclusion 3 allows the assumption that velocity of flow may affect the results of the measurement of susceptibility of alloys to SCC by using the slow strain rate technique.

No definite conclusion can be made as to whether compressive stresses in the surface layer of the ground specimen are responsible for the noble shift of the potential. First, because the magnitude of the compressive stresses resulting from the mechanical method of sample preparation can be different in flat and inner cylindrical surfaces. Second, the deformed surface layer resulting from grinding could get dissolved during the period of time required for achieving stable conditions.

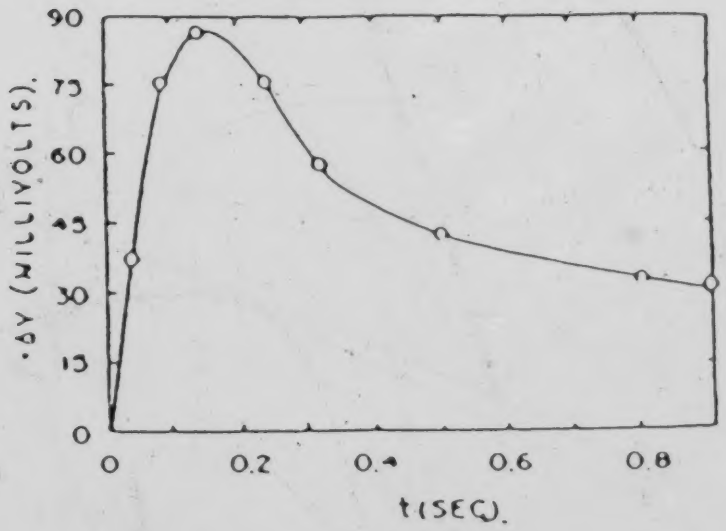

Figure 1. The electrode potential transient of copper in distilled water (ref. 20).

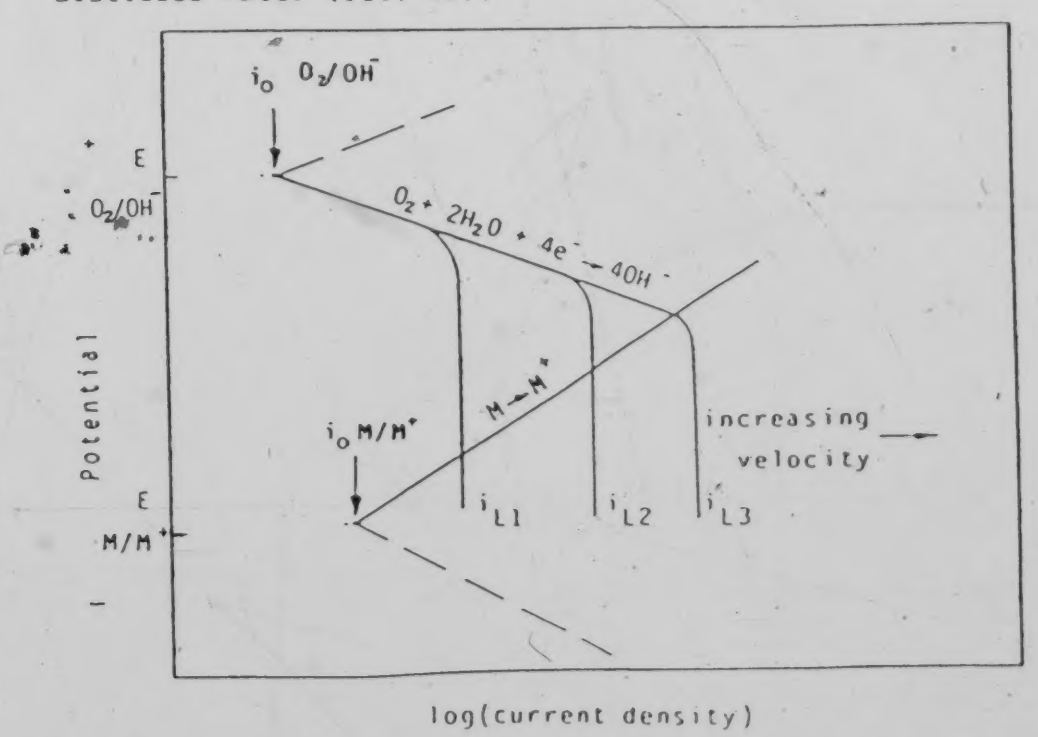

Figure 2. Effect of velocity of flow on the electrochemical behaviour of metal corroding with a diffusion controlled cathodic reaction (ref. 32).

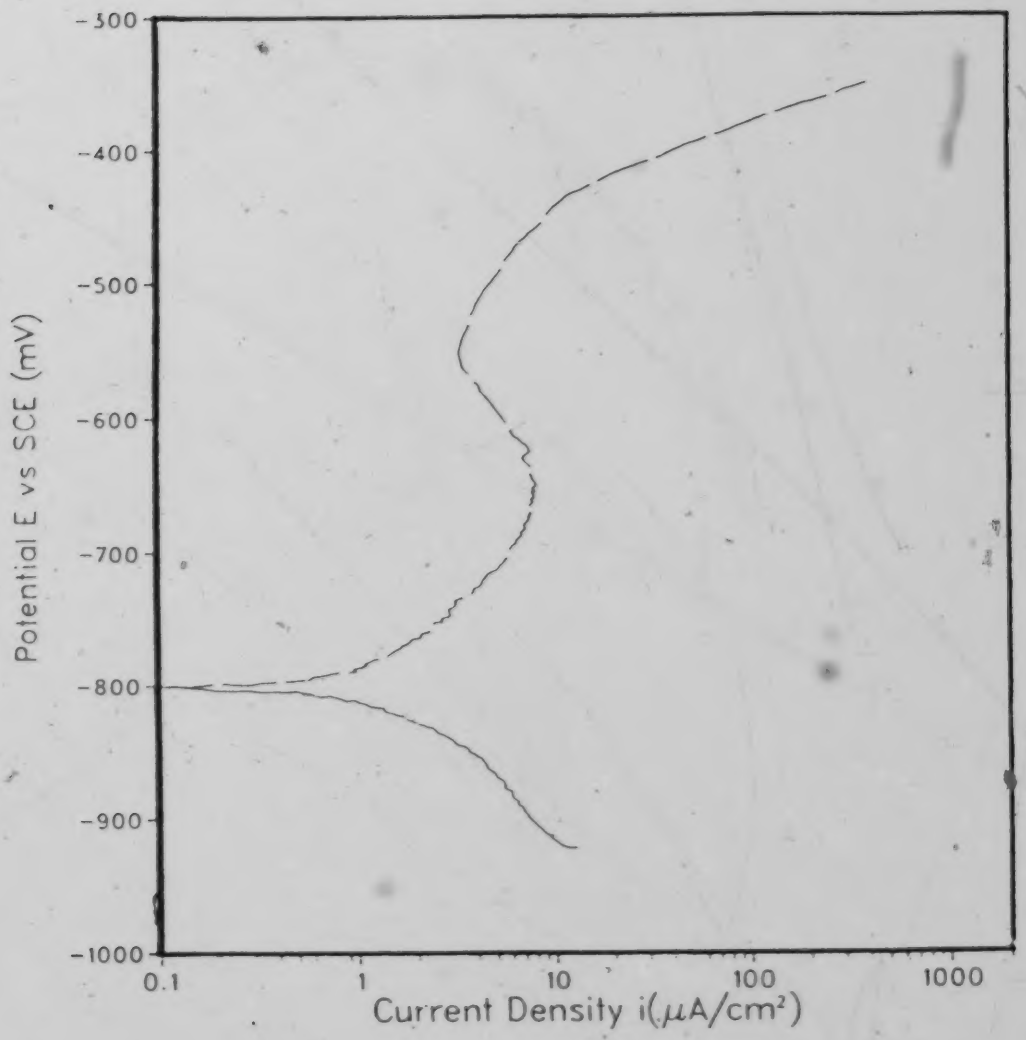

Figure 3. Polarization curves for 1025 steel in 3% NaCl solution at room temperature.

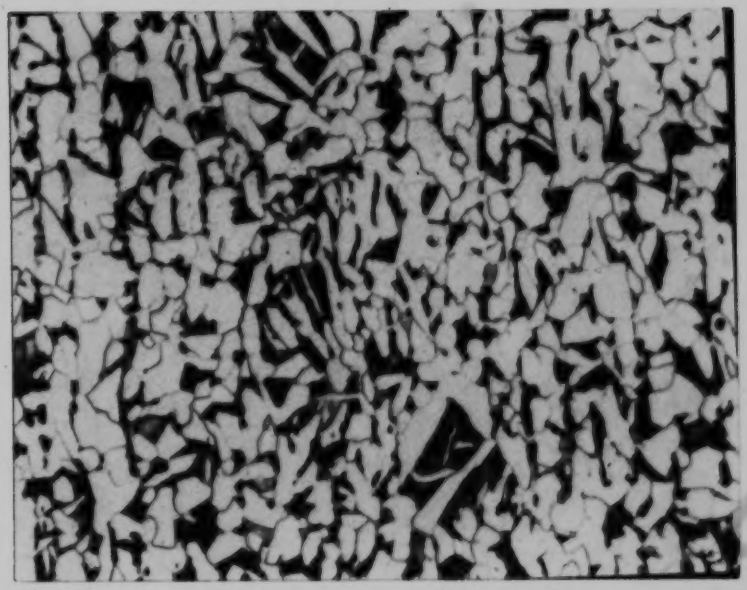

Figure 4. Microstructure of 1025 steel magnified 200 times.

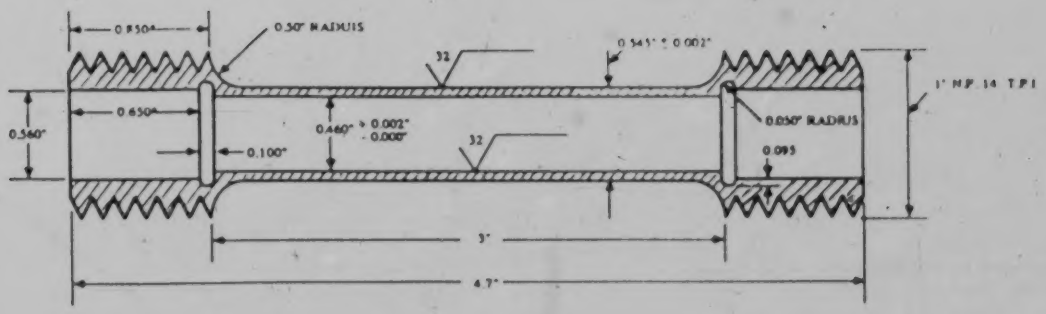

Figure 5. The test specimen.

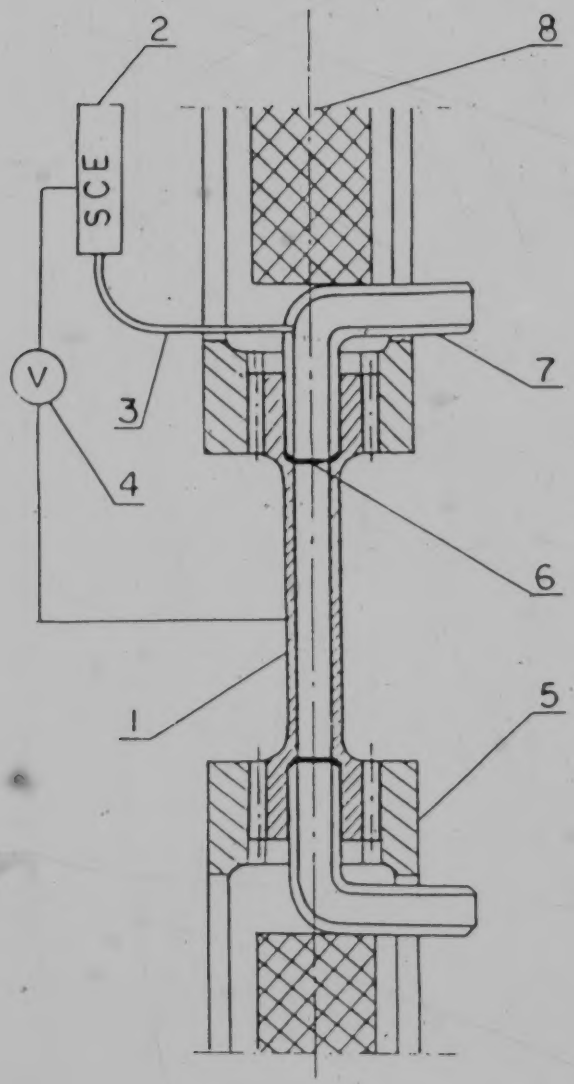

1. Test specimen.
2. Standard electrode.
3. Luggin capillary.
4. Voltmeter.
5. Tensile machine grip.
6. Rubber washer.
7. Plastic elbow.
8. Plastic insert.

Figure 6. The test corrosion cell.

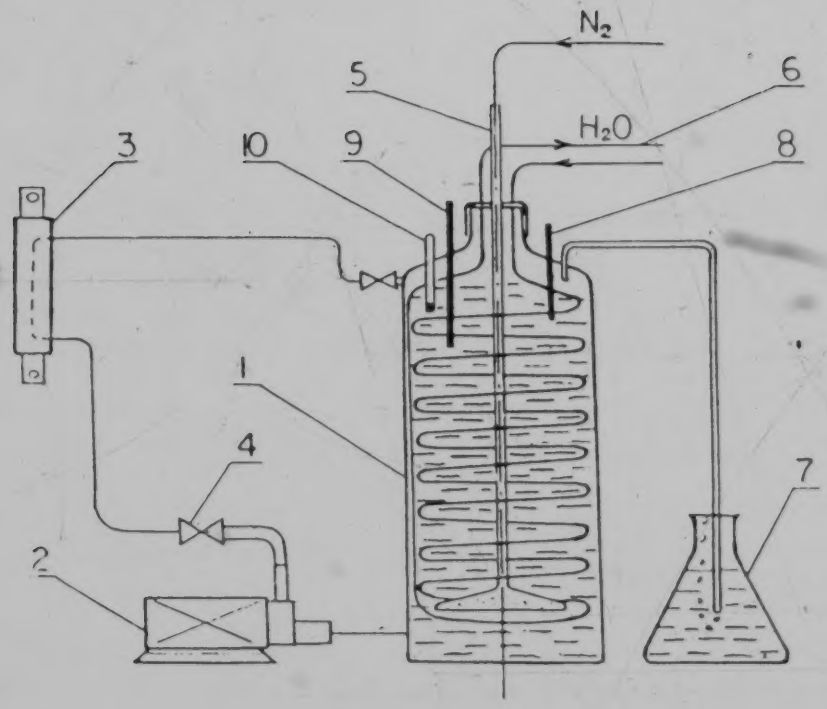

1. Solution tank.
2. Electromagnetic pump.
3. Test cell.
4. Flow valve.
5. Nitrogen line filter.
6. Cooling coil.
7. Nitrogen overflow.
8. pH meter.
9. Thermometer.
10. Oxygen meter.

Figure 7. Schematic drawing of experimental apparatus.

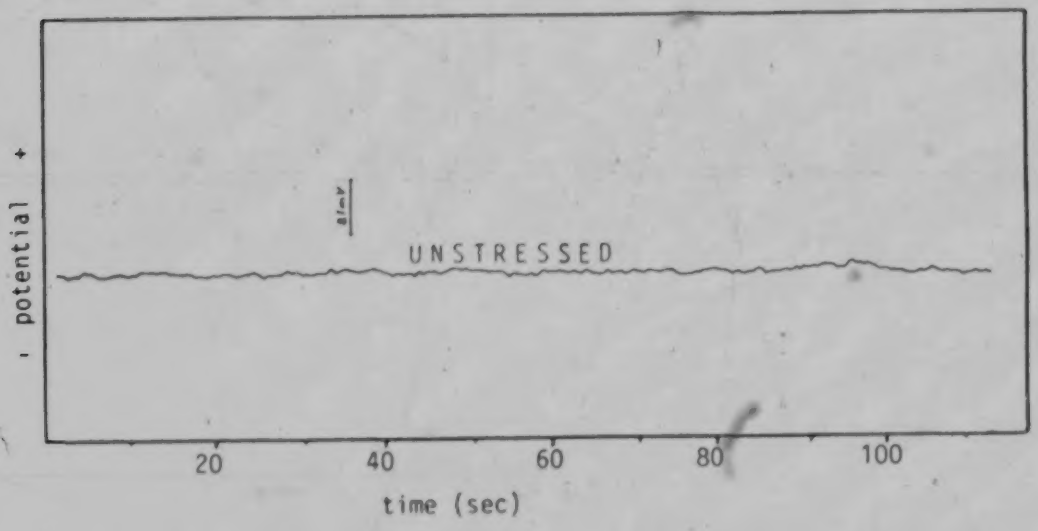

Figure 8. Stability of the corrosion potential at steady conditions in stagnant solution.

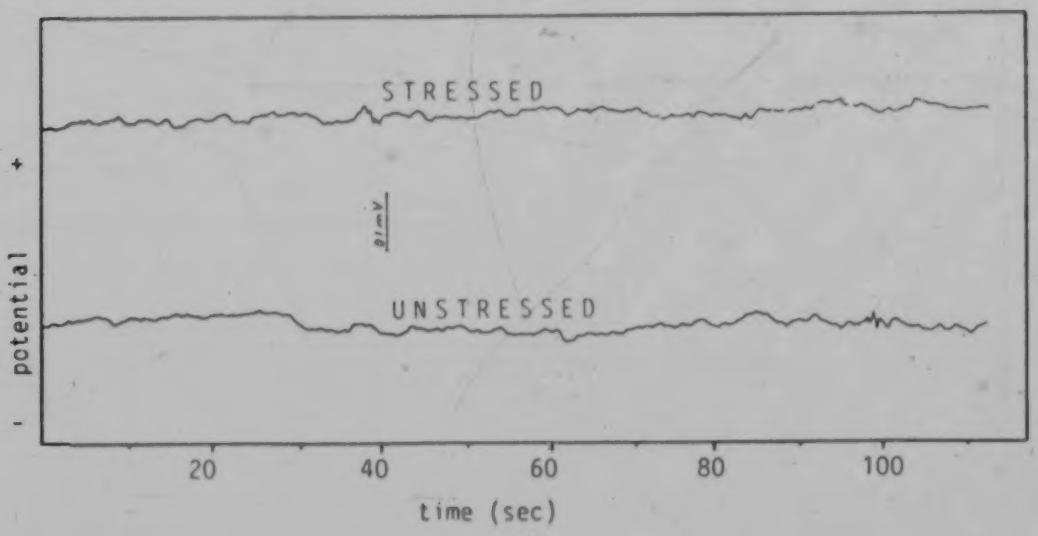

Figure 9. Stability of the corrosion potential at steady state conditions in flowing solution at random velocity.

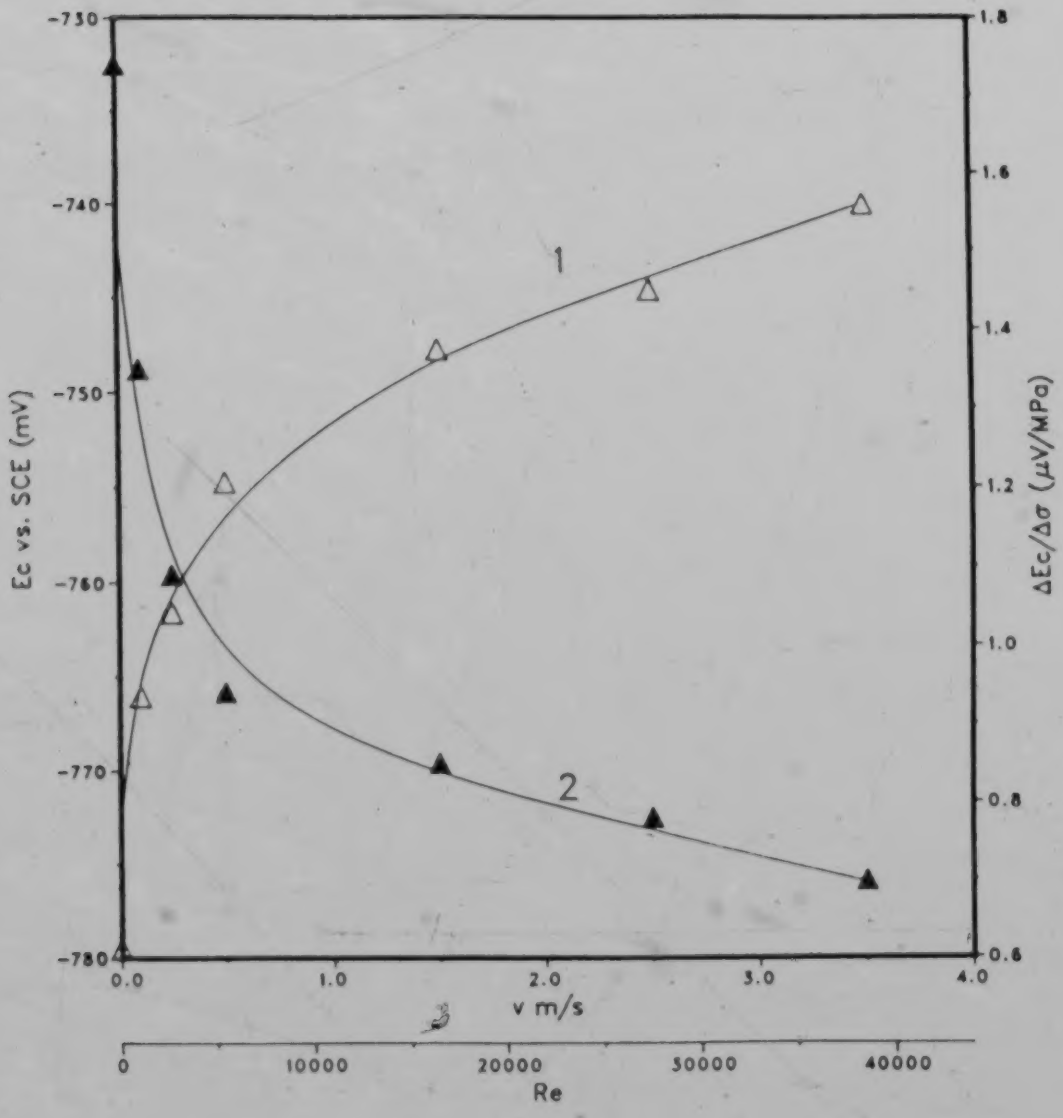

Figure 10. Effect of velocity of flow on:

1. Corrosion potential of 1025 steel in 3% NaCl solution.
2. Slope value of potential/stress lines.

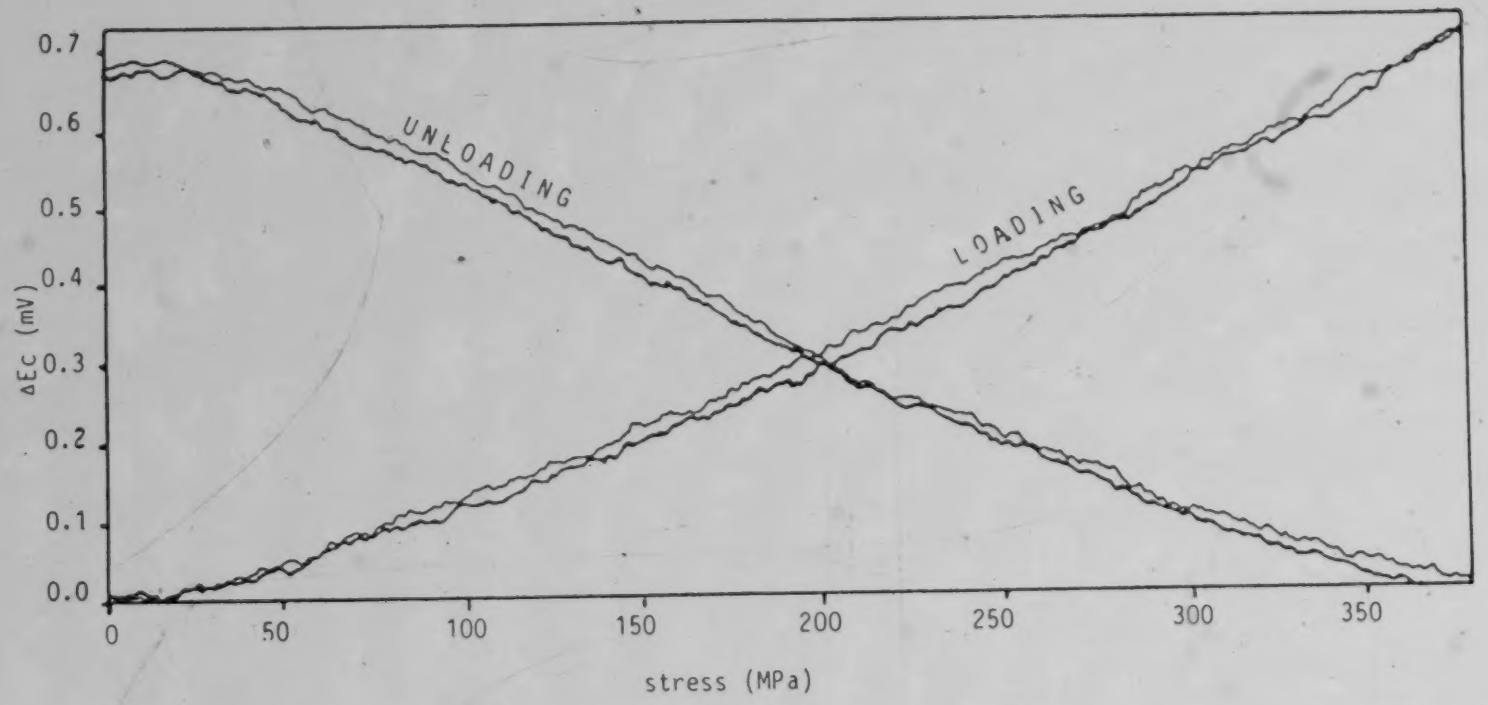

Figure 11. Effect of tensile stress on corrosion potential of 1025 steel in 3% NaCl solution.(Velocity of flow: 0.0 m/s, rest potential:-779.5 mV)

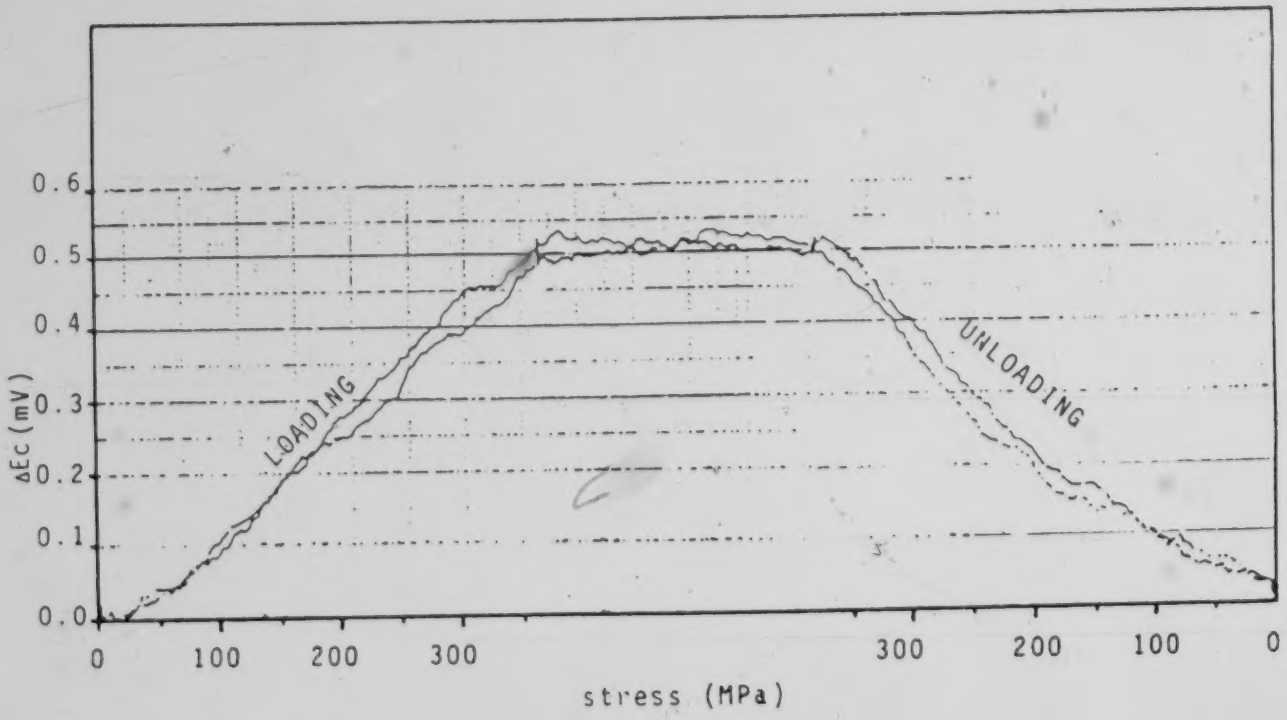

Figure 12. Effect of tensile stress on corrosion potential of 1025 steel in 3% NaCl solution.(Velocity of flow: 0.1 m/s, rest potential:-766.0 mV)

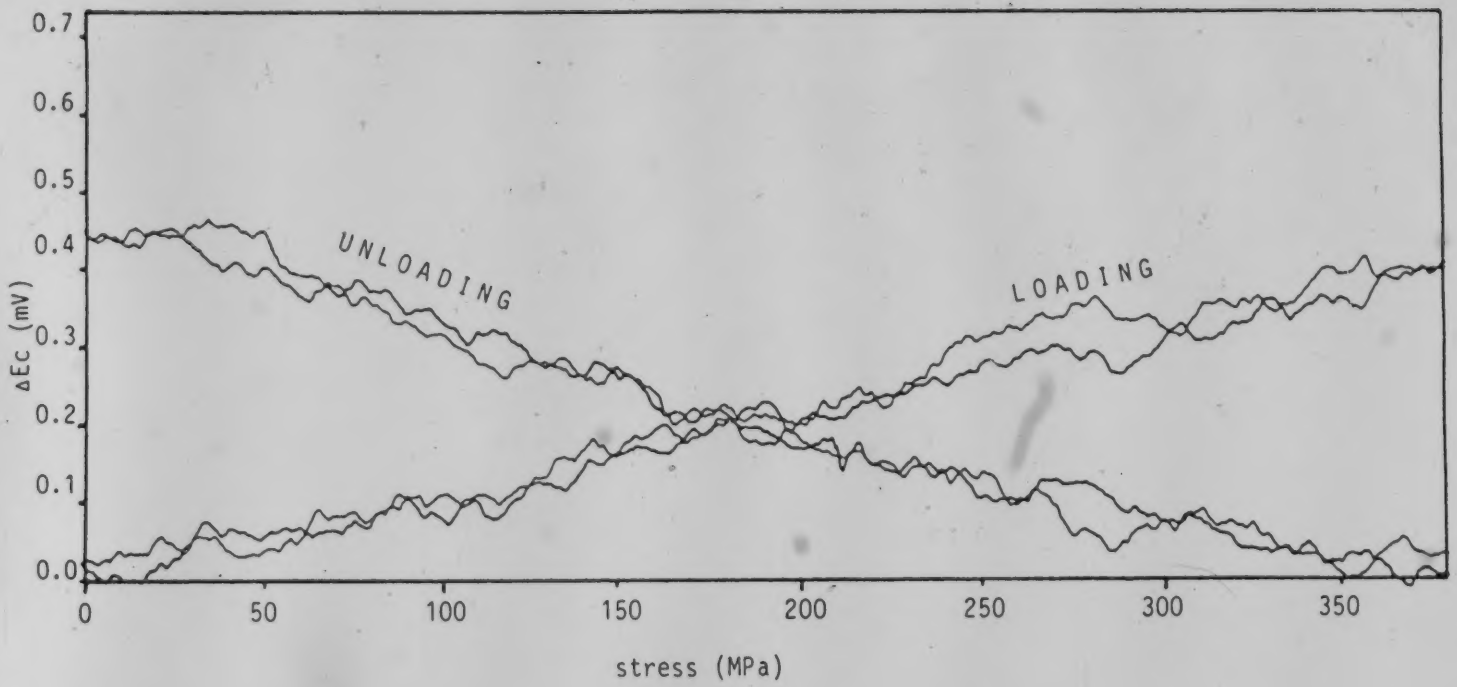

Figure 13. Effect of tensile stress on corrosion potential of 1025 steel in 3% NaCl solution.(Velocity of flow: 0.25 m/s, rest potential:-758.9 mV)

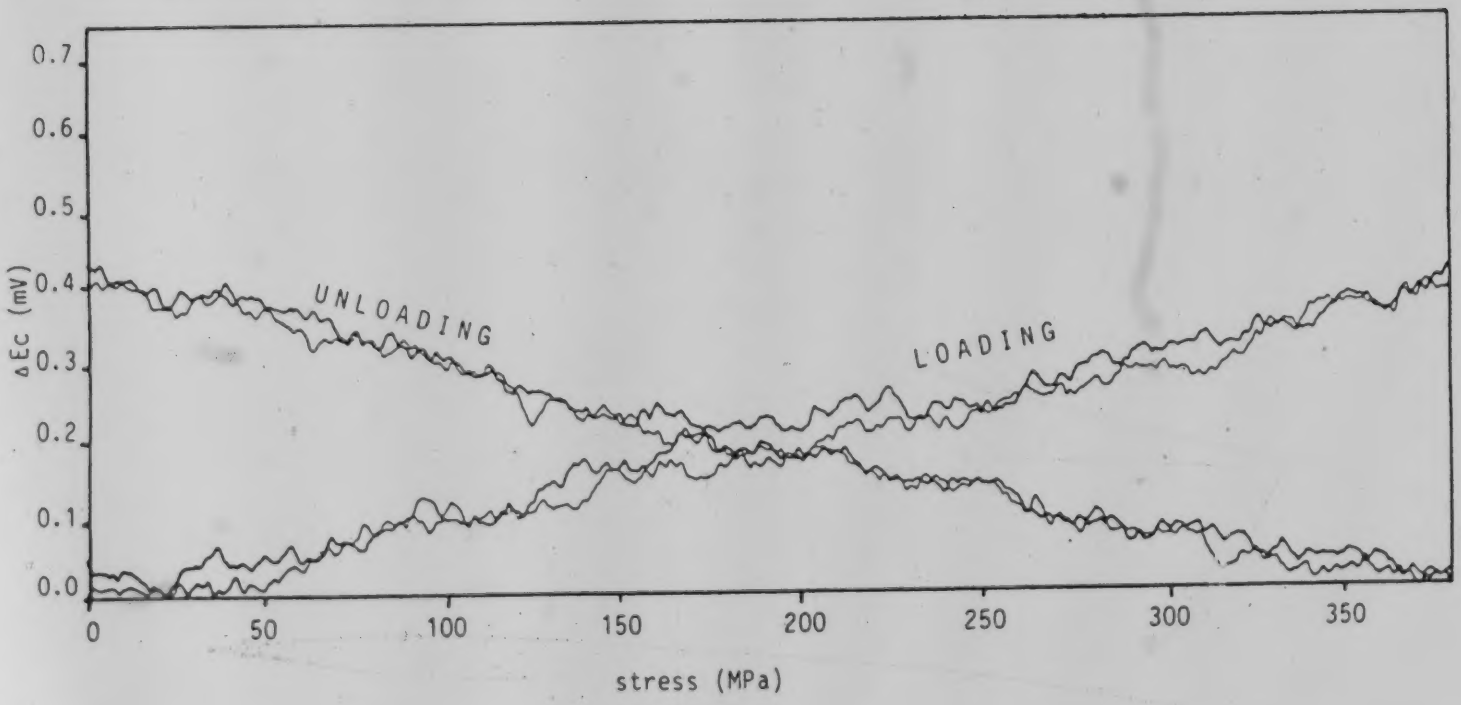

Figure 14. Effect of tensile stress on corrosion potential of 1025 steel in 3% NaCl solution.(Velocity of flow: 0.5 m/s, rest potential:-754.7 mV)

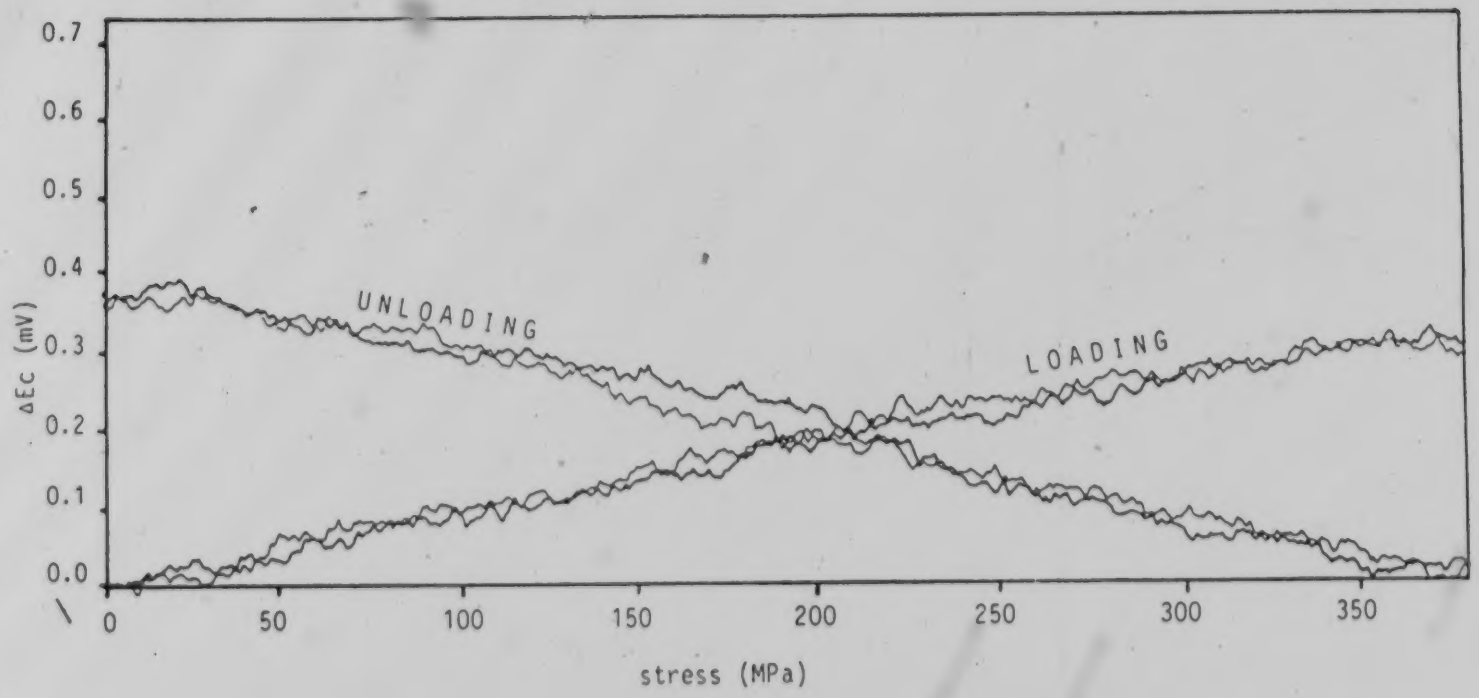

Figure 15. Effect of tensile stress on corrosion potential of 1025 steel in 3% NaCl solution.(Velocity of flow: 1.5 m/s, rest potential:-747.7 mV)

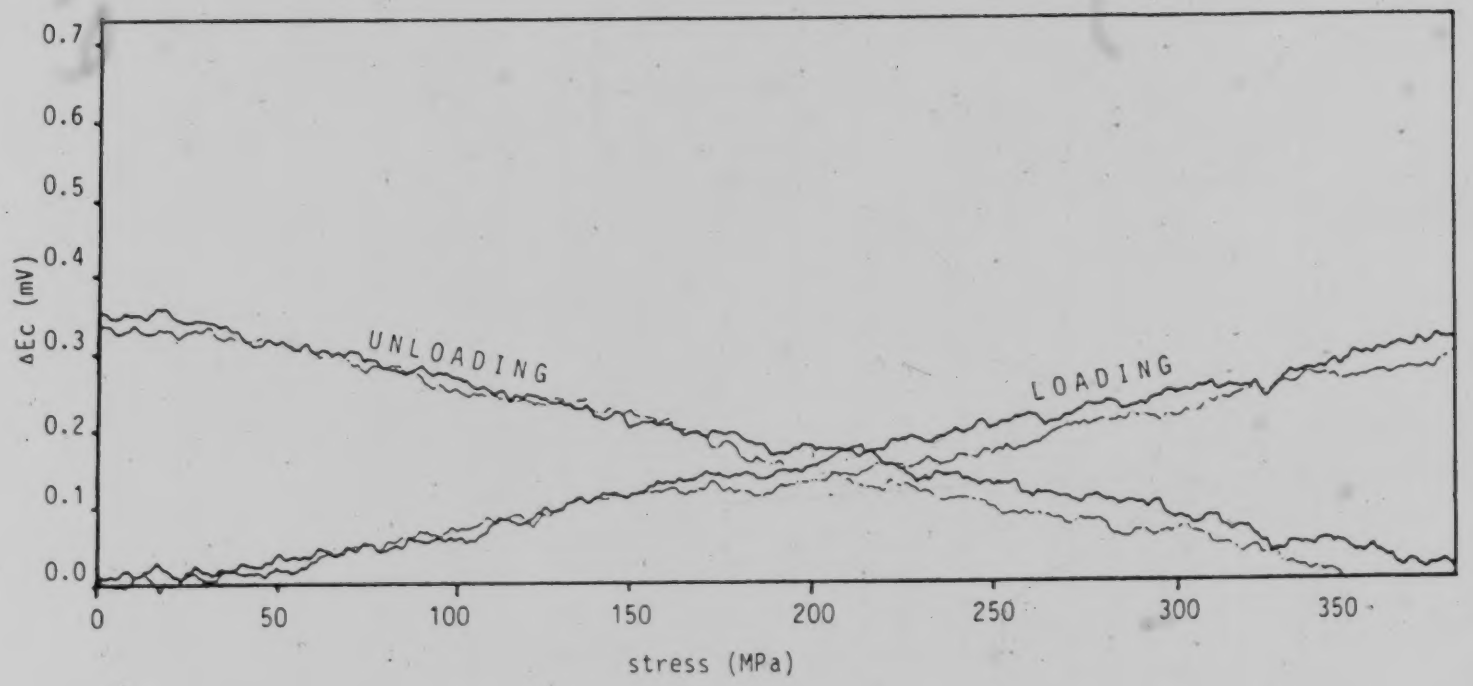

Figure 16. Effect of tensile stress on corrosion potential of 1025 steel in 3% NaCl solution.(Velocity of flow: 2.5 m/s, rest potential:-744.5 mV)

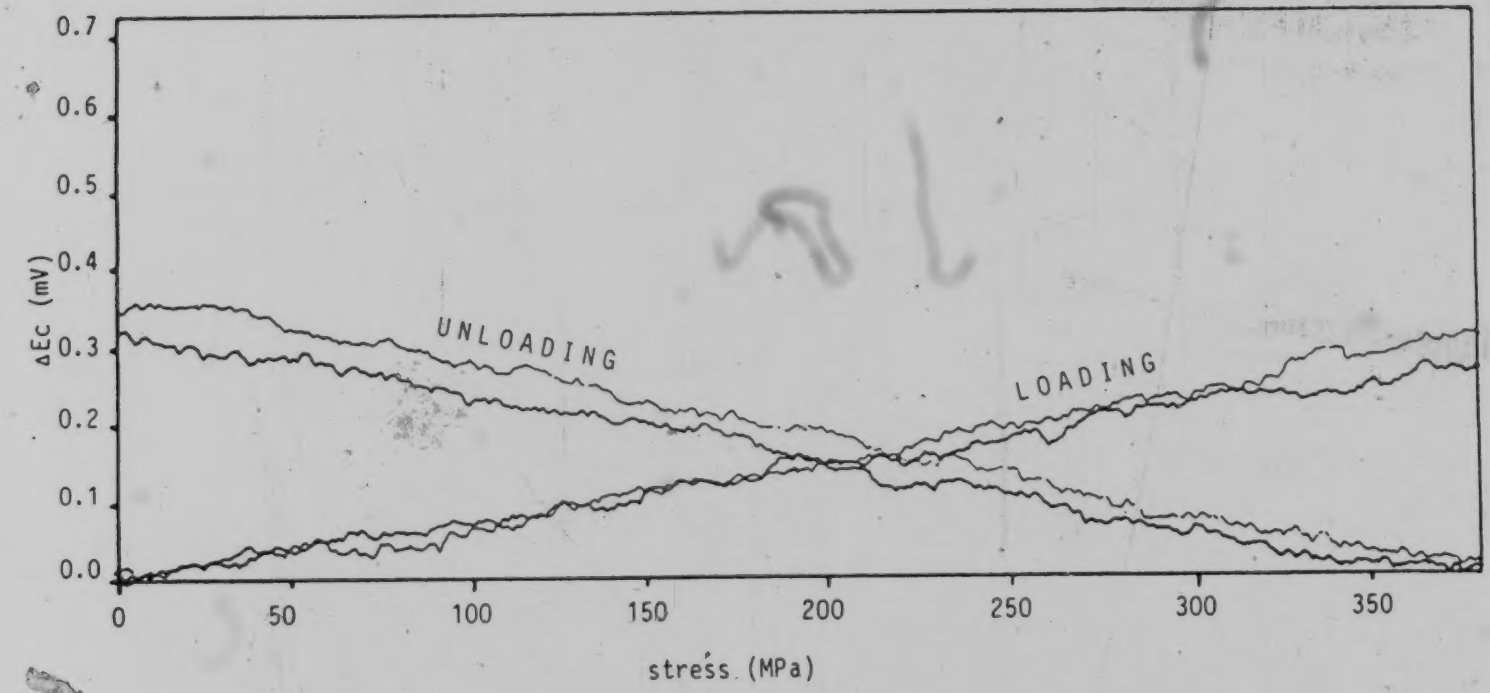

Figure 17. Effect of tensile stress on corrosion potential of 1025 steel in 3% NaCl solution.(Velocity of flow: 3.5 m/s, rest potential:-740.0 mV)

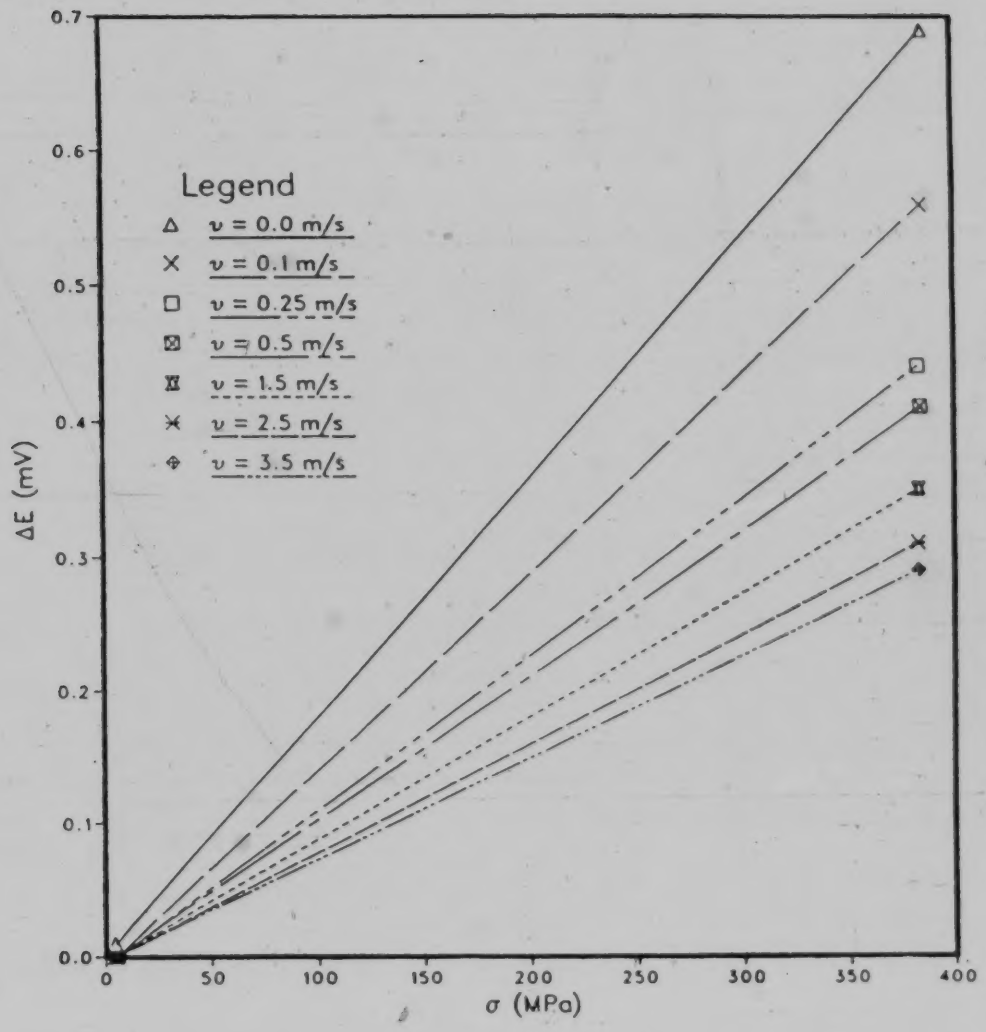

Figure 18. Effect of tensile stress on corrosion potential of 1025 steel in 3% NaCl solution at various velocities of flow.

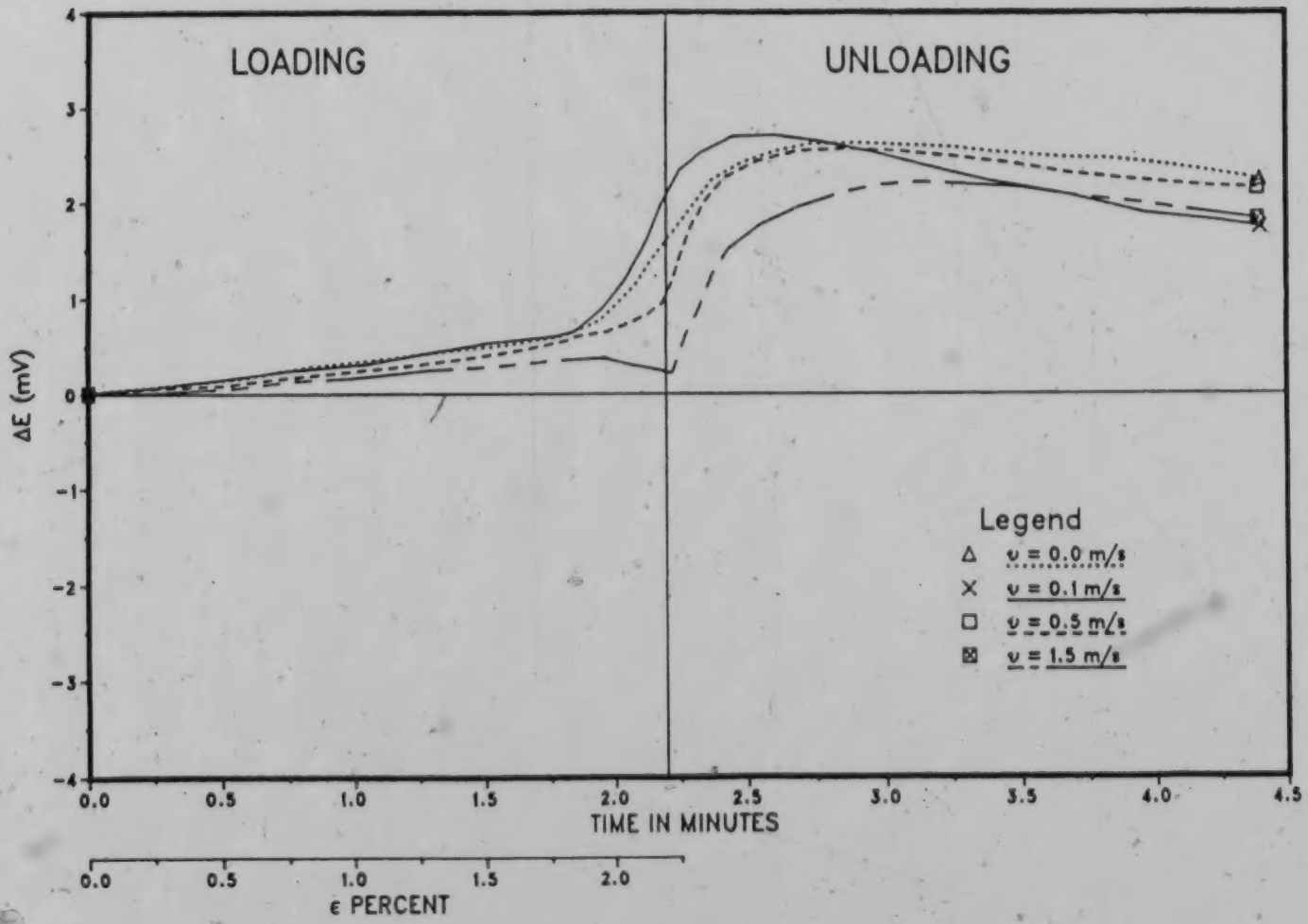

Figure 19. Potential change during the first straining cycle at various flow rates.

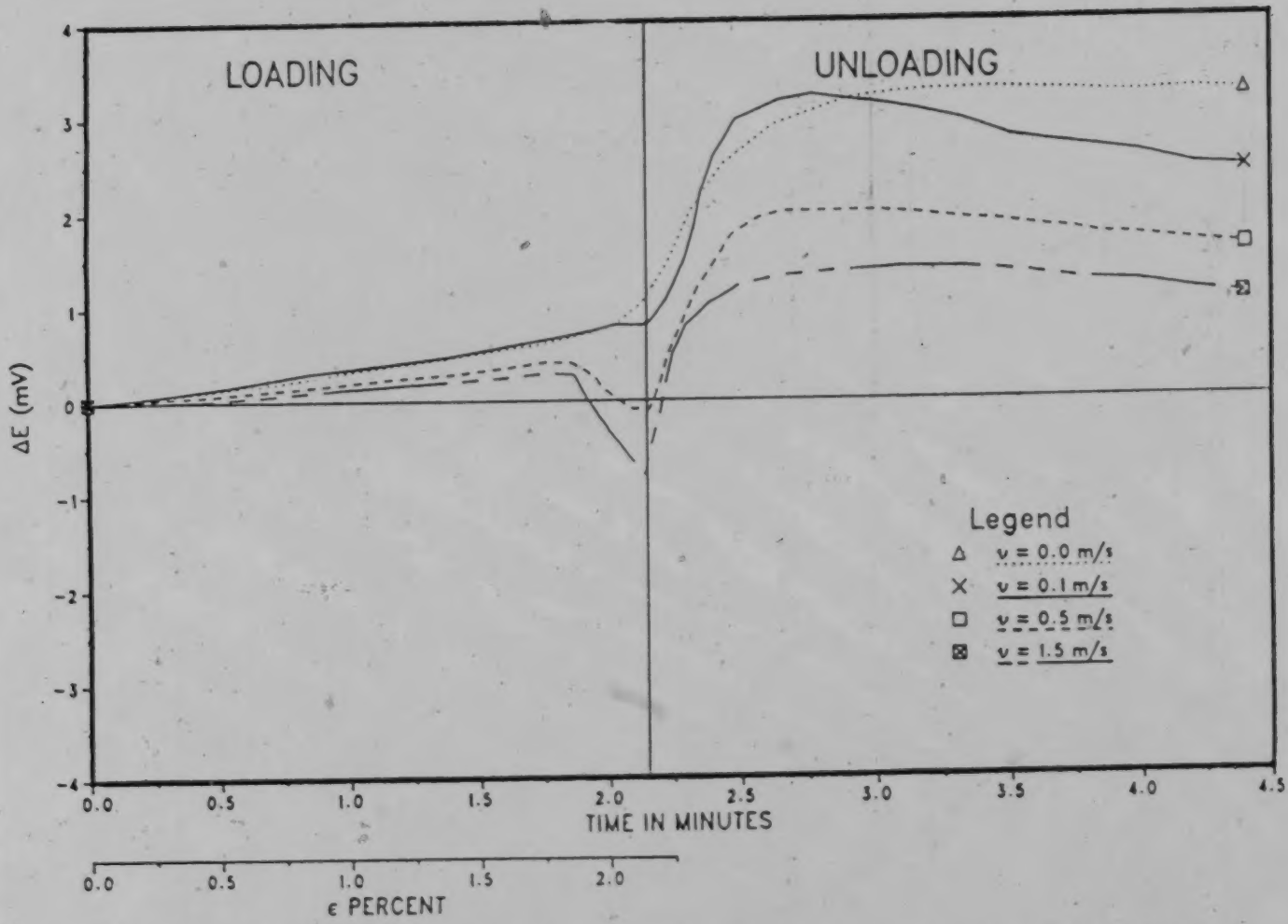

Figure 20. Potential change during the second straining cycle at various flow rates.

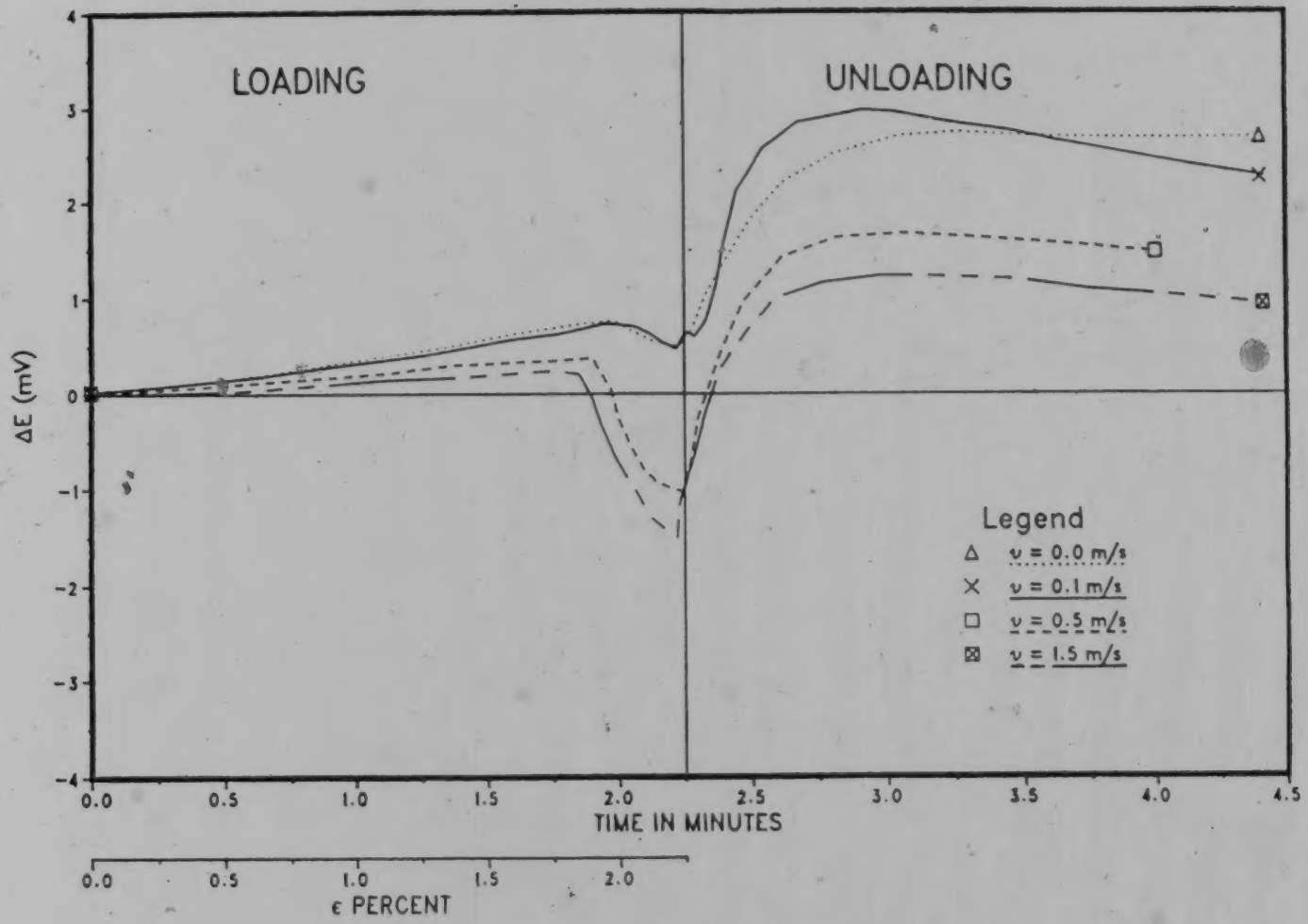

Figure 21. Potential change during the third straining cycle at various flow rates.

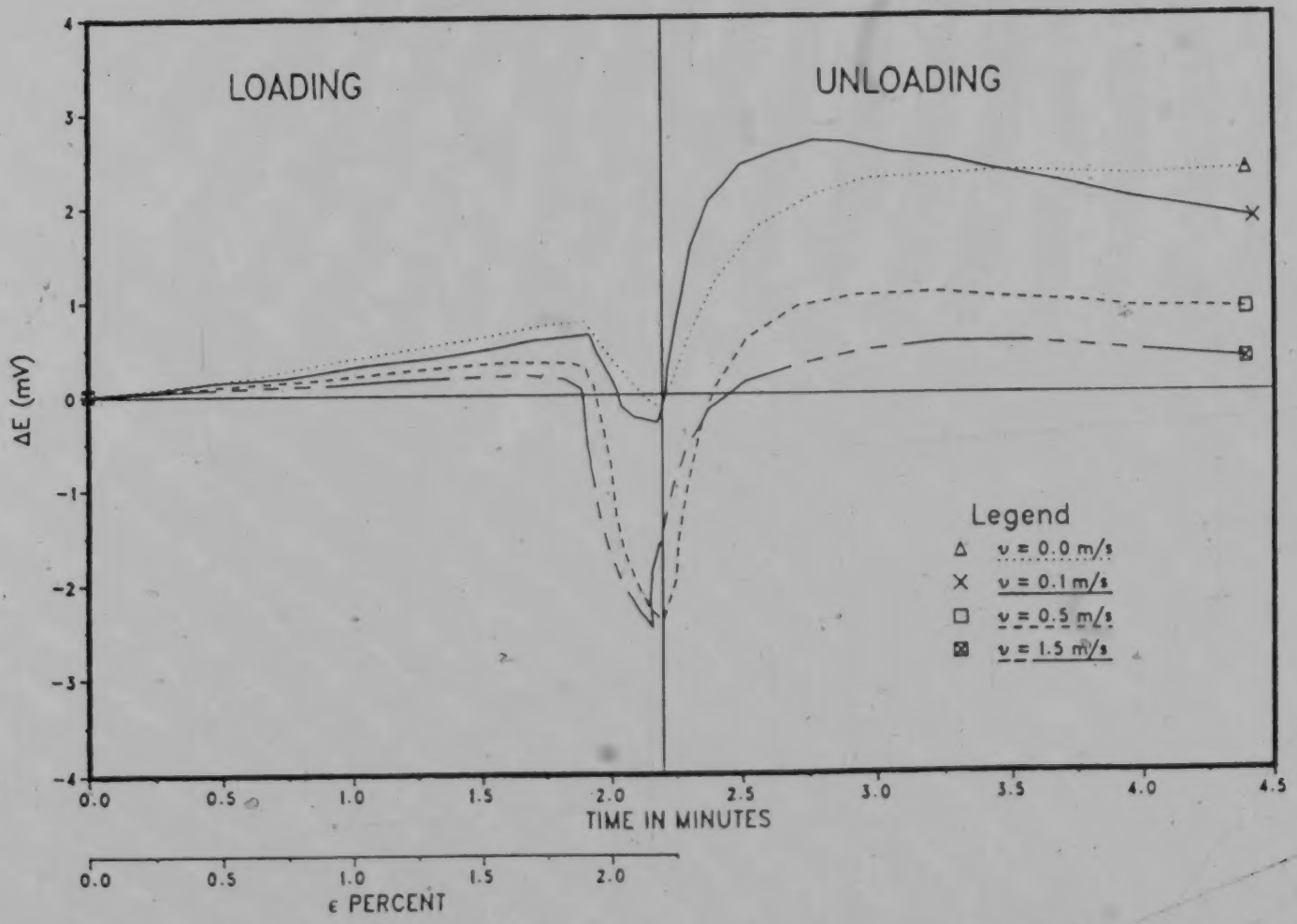

Figure 22. Potential change during the fourth straining cycle at various flow rates.

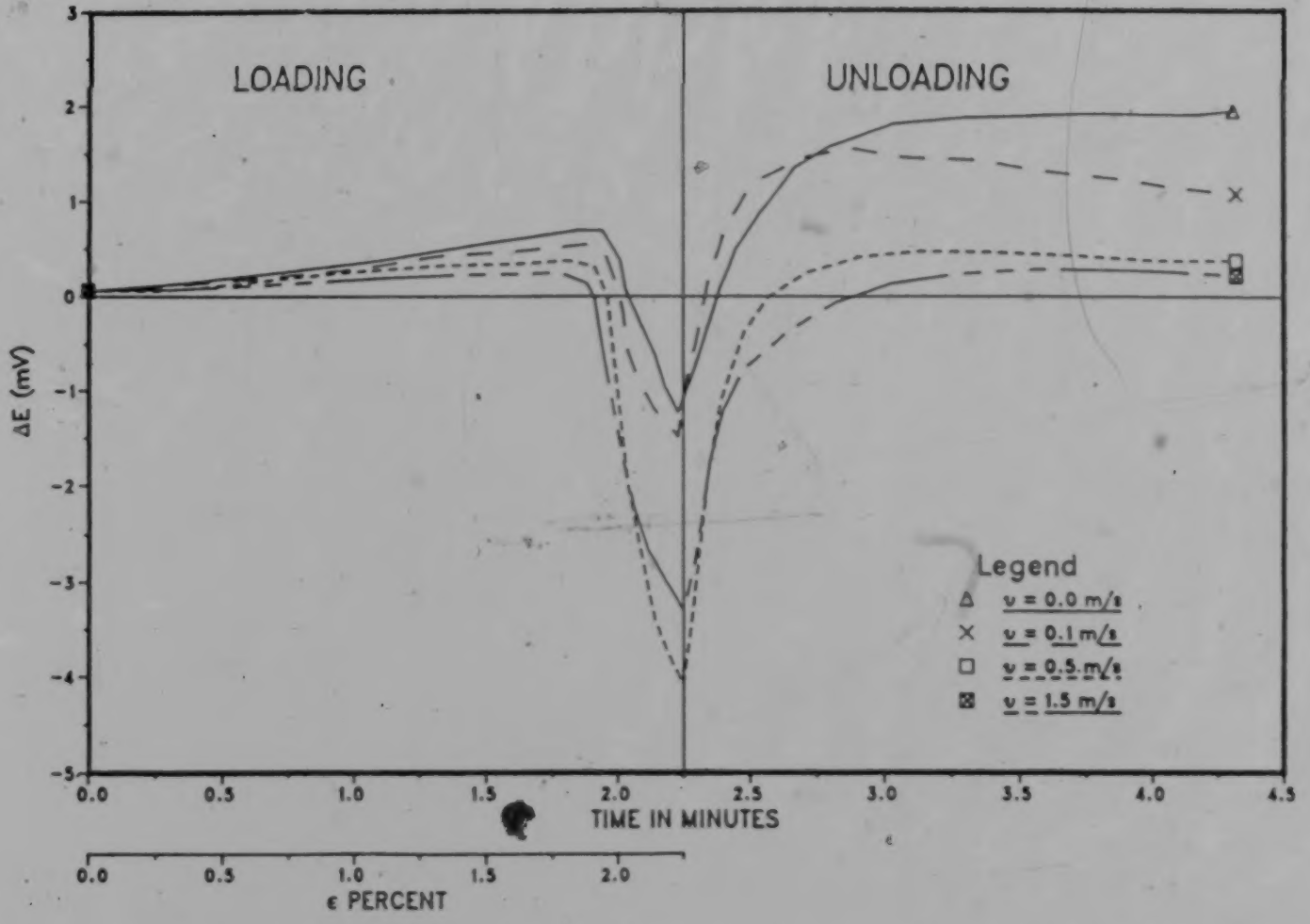

Figure 23. Potential change during the fifth straining cycle at various flow rates.

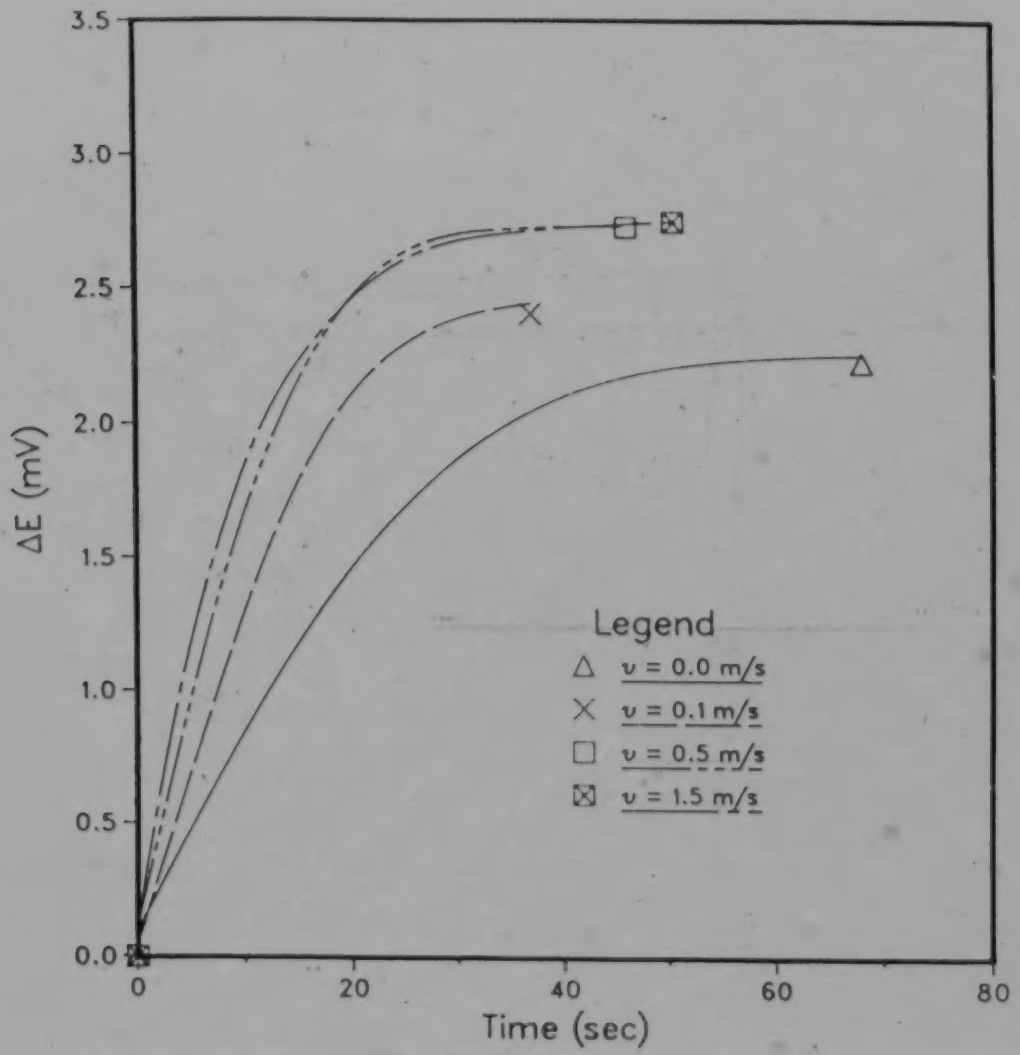

Figure 24. Potential decay curves for 1025 steel in 3% NaCl solution at various velocities of flow for third straining cycle (up to the maximum potential).

REFERENCES

1. Choi, E., Beck, F.H., Szklarska-Smialowska, Z., Macdonald, D.D. The effect of fluid flow on the stress corrosion cracking of ASTM A508 CL2 steel and A151 type 304 stainless steel in high temperature water. CORROSION, Vol.40, No.2: p.76-85, February 1982.
2. Hickling, J. The effect of fluid flow on the stress corrosion cracking of ASTM A508 CL2 steel in high temperature water. CORROSION, Vol.40, No.1: p.36-37, January 1984.
3. Kestin, J. A COURSE IN THERMODYNAMICS. McGraw-Hill Book Company, New York, Vol.1, p.340, 1979.
4. Swalin, R.A. THERMODYNAMICS OF SOLIDS. John Wiley and Sons, Inc., New York. London. p.25, 1962.
5. Beynon, J.G., Butler, G., Francis, P.E., McKie, A.S. The influence of oxygen on the corrosion potential of a number of metals at 150 and 250 C. High Temperature High Pressure Electrochemistry in Aqueous Solution. NATIONAL ASSOCIATION OF CORROSION ENGINEERS. Houston, 1976, p.430.
6. Flood, E.A. Some thermodynamic considerations of the effects of stress on metal electrode potential. CANADIAN J. CHEM, Vol.36: p.1332-1337, 1958.
7. Huffstutler, M.C. Fundamental considerations of stress corrosion. CORROSION, Vol.19: p.423t-426t, December 1963.
8. Walker, W.H., Dill, C. The effect of stress upon the

electromotive force of soft iron. THE ELEVENTH GENERAL MEETING OF THE AMERICAN ELECTROCHEMICAL SOCIETY, in Philadelphia. Pa. p.153, May 3, 1907.

9. Murata, T., Staehle, R.W. Theory and application of straining electrode. PROC. OF THE FIFTH INTER. CONGRESS ON METALLIC CORROSION. Tokyo, Japan, p.513, 1972.
10. Simnad, M.T., Evans, U.R. The influence of stress upon the electrode potential and polarization of iron and steel in acid solution. FARADAY SOCIETY TRANS. Vol.43, No.327: p.175-186, November 1950.
11. Taylor, G.I., Yarrow, F.R.S., Quinney, H. The latent energy remaining in a metal after cold working. PROC. OF THE ROYAL SOCIETY, Vol.143A: p.307, 1934.
12. Bohnenblust, H.F., Duwez, P. Some properties of a mechanical model of plasticity. JOURNAL OF APPLIED MECHANICS, Vol.15: p.222, 1948.
13. Hoar, T.P. The anodic behaviour of metals. MODERN ASPECTS OF ELECTROCHEMISTRY, No.2: p.262, Butterworths, London, 1959.
14. Howard, D., Pyle, T. The dissolution of atoms from steps on a metal surface. PHIL. MAG. Vol.14: p.1179-1189, 1966.
15. Hurlen, T. Kinetics of metal/metal-ion electrodes: iron, copper, zinc. ELECTROCHEMICA ACTA, Vol.7: p.663-668, 1962.
16. Burton, W.K., Cabrera, N., Frank, F.C. The growth of crystals and the equilibrium structure of their

surfaces. PHIL. TRANS. Vol.243A: p.299, 1951.

17. Doremus, R.H., Roberts, B.W., Turnbull, D. Growth and perfection of crystals. PROC. OF INTERNATIONAL CONFERENCE ON CRYSTRAL GROWTH, held at Cooperstown, New York, 1958, Wiley, New York, 1958.
18. Fleischmann, M., Thirsk, H.R. Anodic electrocrystallization. ELECTROCHEMICA ACTA, Vol.2: p.22-49, 1960.
19. Windfeldt, A. Anodic dissolution of active metals during plastic flow: iron and nickel. ELECTROCHEMICA ACTA, Vol.9: p.1139-1147, 1964.
20. Funk, A.G., Giddings, J.C., Christensen, C.J., Eyring, H. Strain electrometry and corrosion I. General considerations on interfacial electrical transients. PROC. OF NATIONAL ACADEMY OF SCIENCE, Vol.43: p.421, 1957.
21. Funk, A.G., Giddings, J.C., Christensen, C.J., Eyring, H. Strain electrometry and corrosion II. Chemical effects with copper electrodes. JOURNAL OF PHYSICAL CHEMISTRY, Vol.61: p.1179, 1957.
22. Giddings, J.C., Funk, A.C., Christensen, C.J., Eyring, H. Strain electrometry and corrosion, IV. Film property and strain potential. JOURNAL OF THE ELECTROCHEMICAL SOCIETY, Vol.106: p.91, 1959.
23. Evans, U.R., Simnad, M.T. The mechanism of corrosion fatigue of mild steel. PROC. OF ROYAL SOCIETY, Vol.188A: p.372, 1946-47.

24. Tan, S., Nobe, K. Galvanic stress potentials of metals. CANADIAN JOURNAL OF CHEMISTRY, Vol.41: p.495, 1963.

25. Fryxell, R.E., Nachtrieb, N.H. Effect of stress on metal electrode potentials. JOURNAL OF ELECTROCHEMICAL SOCIETY, Vol.99, No.12: p.495, 1952.

26. Nobe, K., Seyer, W.F. Effect of torsional stress on the electrode potential of copper. JOURNAL OF APPLIED PHYSICS, Vol.29, No.12: p.1632, 1958.

27. Foroulis, Z.A., Uhlig, H.H. Effect of cold-work on corrosion of iron and steel in hydrochloric acid. JOURNAL OF THE ELECTROCHEMICAL SOCIETY, Vol.111, No.5: p. 522, 1964.

28. Salvago, G., Fumagalli, G., Sinigaglia, D. The corrosion behaviour of AISI 304L stainless steel in 0.1 M HCl at room temperature -I. CORROSION SCIENCE, Vol.23, No.5: p.507-514, 1983.

29. StÜwe, H.P., Pink, E. Das anodische Verhalten von Metallen wahrend das Zugversuches. ZEITSCHRIFT FUR METALLKUNDE, Vol.76(12): p.772, 1985.

30. Burgess, C.F. The corrosion of iron from an electrochemical standpoint. THE THIRTEENTH GENERAL MEETING OF THE AMERICAN ELECTROCHEMICAL SOCIETY, held at Albany, N.Y. April 30, 1908.

31. Harwood, J.J. The influence of stress on corrosion. CORROSION, Vol.6: p.249, 1950.

32. Simnad, M.T. A review of the electrochemistry of stressed metals. ELECTROCHEMICAL SOCIETY, Vol.97: p.31C,

1950.

33. Fontana, M.G., Greene, N.D. CORROSION ENGINEERING, second edition, McGraw-Hill Book Company, New York, 1978.

34. Levich, V.G. PHYSICOCHEMICAL HYDRODYNAMICS, Prentice-Hall, Inc. Englewood Cliffs, N. J. 1962.

35. Poulson, B. Electrochemical measurements in flowing solutions. CORROSION SCIENCE, Vol.23, No.4: p.391-430, 1983.

36. Vennard, J.K., Street, R.L. ELEMENTARY FLUID MECHANICS, sixth edition, John Wiley & Sons, New York, 1982.

37. Ross, T.K., Hitchen, P.L. Some effects of electrolyte motion during corrosion. CORROSION SCIENCE, Vol.1: p.65-75, 1961.

38. Mahato, B.K., Voora, S.K., Shemilt, L.W. Steel pipe corrosion under flow conditions - I. An isothermal correlation for a mass transfer model. CORROSION SCIENCE, Vol.8: p.173-193, 1968.

39. Lee, T.S., Thiele, E.W., Waldorf, J.M. The effect of sea water velocity on corrosion potential of materials. MATERIALS PERFORMANCE, Vol.23, part 2: p.44, November 1984.

40. ANNUAL BOOK OF ASTM STANDARDS. American Society for Testing and Materials, Philadelphia, Vol.03.02: p.124, 1987.

APPENDIX A. Calculation of temperature change due to thermoelastic effect

Quantities for variables in equation 5 are given as follows:

$T = 300$ K

$\Delta\sigma = 500\times10^{6}$ Nm/m^3

$\alpha = 11\times10^{-6}$ 1/K

$c_p = 24.22$ Joules/mol K

$V = M/\rho$

$M = 0.056$ kg/mol

$\rho = 7.8\times10^{3}$ kg/m^3

$V = 7.18\times10^{-6}$ m^3/mol

Substituting these values in equation 5 we obtain

$$\Delta T = -0.16 \text{ K}$$

APPENDIX B. Thermodynamic calculation of potential change of stressed steel.

For a specimen stressed uniaxially the stored energy per unit volume can be calculated by using the following formula:

$$W = \sigma^2/2\,E$$

where:

W = work done by tensile loading.

σ = stress applied.

E = Young's modulus.

Putting in the following experimental data:

σ = 385 MPa.

E = 205×10^3 MPa.

we obtain:

W = 0.362 Joules/cm^3

Assuming for steel:

ρ = 7.86 g/cm^3

M = 55.85 g/mol

the work done per mole of steel is:

W = 2.57 Joules/mol

Assuming that the process is isothermal and the work done against the surroundings is negligible:

$$W = \Delta G$$

and therefore equation 1 can be written:

$$\Delta E = -W/nF$$

Assuming for steel:

n = 2 moles of e^-/mol of metal

F = 96460 C/mol of e^-

$\Delta E = -0.0133$ mV

For a linear change the slope $\Delta E/\Delta\sigma$ is equal to -0.0346 μV/MPa.

APPENDIX C. Determining the corrosion rate of 1025 steel in 3% NaCl solution.

Converting current density which was determined from Figure 3 into penetration depth per unit time we have:

$$v = \frac{iM}{nF\rho}$$

Putting in the following data:

$i = 1.8\times10^{-3}$ A/m²

$M = 56$ g/mol

$n = 2$ mol e^-/mol of metal

$F = 96460$ C/mol e^-

$\rho = 7.8\times10^{6}$ g/m³

the calculated corrosion rate is 0.241×10^{-3} μm/h.